T.R.
GEBZE TECHNICAL UNIVERSITY
GRADUATE SCHOOL

COMPUTATIONAL INVESTIGATION OF POOL BOILING AROUND DIFFERENT DIAMETER HORIZONTAL TUBES UNDER ATMOSPHERIC AND SUB-ATMOSPHERIC PRESSURE

SİNAN ÖZBÖLGİLİ

A THESIS OF MASTER OF SCIENCE
DEPARTMENT OF MECHANICAL ENGINEERING

ADVISOR: ASSOC. PROF. DR. GAMZE GEDİZ İLİŞ

JUNE 2024

T.R.
GEBZE TECHNICAL UNIVERSITY
GRADUATE SCHOOL

COMPUTATIONAL INVESTIGATION OF POOL BOILING AROUND DIFFERENT DIAMETER HORIZONTAL TUBES UNDER ATMOSPHERIC AND SUB-ATMOSPHERIC PRESSURE

SİNAN ÖZBÖLGİLİ

A THESIS OF MASTER OF SCIENCE
DEPARTMENT OF MECHANICAL ENGINEERING

ADVISOR: ASSOC. PROF. DR. GAMZE GEDİZ İLİŞ

JUNE 2024

T.C.
GEBZE TEKNİK ÜNİVERSİTESİ
LİSANSÜSTÜ EĞİTİM ENSTİTÜSÜ

FARKLI ÇAPLARDAKİ YATAY BORULAR UZERİNDE HAVUZ KAYNAMANIN ATMOSFER VE ATMOSFER ALTI BASINCLARDA SAYISAL İNCELENMESİ

SİNAN ÖZBÖLGİLİ

YÜKSEK LİSANS TEZİ
MAKİNE MÜHENDİSLİĞİ ANABİLİM DALI

DANIŞMAN: DOÇ. DR. GAMZE GEDİZ İLİŞ

HAZİRAN 2024

MASTER of SCIENCE JURY APPROVAL FORM

A thesis submitted by Sinan ÖZBÖLGİLİ, defended on 06/06/2024 before the jury formed with the 03/06/2024 date and 2024/30 numbered decision of the GTU Graduate Administration Board, has been accepted as a MASTER of SCIENCE thesis in the Department of Mechanical Engineering

JURY

MEMBER

(THESIS ADVISOR) : Assoc. Prof. Dr. Gamze GEDİZ İLİŞ

MEMBER : Asst. Prof. Salih Özen ÜNVERDİ

MEMBER : Assoc. Prof. Dr. Sertaç ÇADIRCI

APPROVAL

Gebze Technical University Graduate Administration Board

…..…/…..…/..…… date and ……/…….. numbered decision.

SIGNATURE/SEAL

ABSTRACT

The boiling method is extensively employed across various industries due to its commendable heat transfer efficacy. Its applications span a wide range, including deployment within utilization within nuclear reactors, integration within electronic systems, incorporation within boiler systems, and diverse cooling applications. In this study, the details of nucleate pool boiling are elucidated, particularly emphasizing the phenomenon of boiling on horizontal tubes. The simulation conducted in ANSYS Fluent software focuses on a horizontal tube immersed in a water tank. Its primary objective is to numerically analyze the pool boiling heat transfer from a horizontally heated copper tube, considering various tube diameters (5 mm. 10 mm, 15 mm, 20 mm) under atmospheric and sub-atmospheric pressures (101 kPa, 47 kPa, 20 kPa, 7.4 kPa, 2.3 kPa). To accomplish this, the simulation employs the Eulerian-Eulerian along with the Rensselaer Polytechnic Institute boiling model, allowing for the replication of the boiling process and the prediction of heat flux and pool boiling heat transfer coefficient within the pool-boiling chamber. Additionally, bubble behaviors have been examined based on different tube geometries and varying pressure conditions. During the evaluation of results, insights from both computational fluid dynamic (CFD) studies conducted with different methods in the literature and experimental research have been utilized to determine the logical framework of the findings. As the ambient pressure decreases, or in other words, as the system is vacuumed, the heat flux generated on the pipe decreases. Similarly, when the diameter of the pipe is increased, a significant decrease in heat is observed.

Keywords: Boiling, Euler Model, Bubble Behavior, Sub-Atmospheric, Numerical Simulation,CFD

ÖZET

Havuz kaynama yöntemi, ısı transferi açısından önemli bir etkinlik sergileyerek çeşitli endüstrilerde yaygın bir şekilde kullanılan bir tekniktir. Bu teknik, nükleer reaktörlerden elektronik sistemlere, kazan sistemlerinden çeşitli soğutma uygulamalarına kadar geniş bir uygulama yelpazesine sahiptir. Bu çalışmada, özellikle yatay borulardaki kaynama fenomenine odaklanılarak nükleat havuz kaynamasının ayrıntıları açıklanmıştır. Simülasyon çalışması, bir su tankına batırılmış yatay bir boru üzerinde gerçekleştirilmiştir ve ANSYS Fluent yazılımı kullanılarak yapılmıştır.

Bu çalışmanın temel amacı, farklı boru çapları (5 mm, 10 mm, 15 mm, 20 mm) altında atmosferik ve atmosfer altı basınçlarda (101 kPa, 47 kPa, 20 kPa, 7.4 kPa, 2.3 kPa) sayısal olarak analiz etmek için bir yatay ısıtılmış bakır borudan havuz kaynaması ısı transferini araştırmaktır. Simülasyon, Euler-Euler ve Rensselaer Polytechnic Institute kaynama modeli kullanılarak gerçekleştirilmiştir. Bu modelleme, kaynama sürecini doğru bir şekilde analiz etmeye ve havuz kaynaması odasında ısı akısı ile havuz kaynama ısı transfer katsayısını tahmin etmeye olanak sağlar.Ayrıca, farklı boru geometrileri ve değişen basınç koşullarına dayanarak kabarcık davranışları incelenmiştir. Sonuçların değerlendirilmesi sırasında, literatürde farklı yöntemlerle yapılan hesaplamalı akişkanlar dinamigi (HAD) çalışmalarından ve deneysel araştırmalardan elde edilen veriler kullanılarak bulguların mantıklı bir çerçevesi oluşturulmuştur.

Çalışmanın sonuçlarına göre, ortam basıncının azalmasıyla, yani sistemin vakumlanmasıyla, boru üzerinde oluşan ısı akısı azalmaktadır. Benzer şekilde, boru çapının artmasıyla, ısı akısında önemli bir düşüş gözlenmektedir. Bu bulgular, endüstriyel sistemlerin tasarımında ve optimize edilmesinde önemli bir rol oynayabilir ve gelecekteki çalışmalar için değerli bir referans noktası sağlayabilir.

Anahtar Kelimeler: Kaynama, Euler Model, Kabarcık Davranışı, Atmosfer Altı, Sayısal Simülasyon, HAD

ACKNOWLEDGEMENTS

I am profoundly thankful for the unwavering support and guidance of my advisor, Assoc. Prof. Gamze GEDIZ ILIS, throughout my master's program. Her expertise and patience have been invaluable, playing a pivotal role in the success of this thesis.
Enormous appreciation for my friends and family for their steadfast love and support, guiding me through this transformative journey.

TABLE OF CONTENTS

	Page
ABSTRACT	v
ÖZET	vi
ACKNOWLEDGEMENTS	vii
TABLE OF CONTENTS	viii
LIST OF SYMBOLS AND ABBREVIATIONS	x
LIST OF FIGURES	xi
LIST OF TABLES	xiii
1. INTRODUCTION	1
2. POOL BOILING	3
2.1. Pool Boiling Regimes	3
2.1.1. Natural Convection Pool Boiling	3
2.1.2. Nucleate Pool Boiling	4
2.1.3. Transition Pool Boiling	5
2.1.4. Film Pool Boiling	5
2.2. Forces on Bubble and Behavior of Bubble	5
2.3. Heat Transfer Mechanism	7
3. LITERATURE REVIEW	10
3.1. Experimental and Numerical Studies	10
3.2. Heat Flux Correlations in Literature	11
4. NUMERICAL MODELING	14
4.1. Problem Definition	14
4.2. Geometry and Mesh	14
4.3. Governing Equations	16
4.4. Numerical Method	20
4.5. Boundary Conditions	20
4.6. Properties of Working Fluids	22
5. MODEL VALIDATION	23
6. RESULTs and DiscussIon	25
6.1. Bubble Forming on Horizontal Tube	25
6.2. Boiling Around Horizontal Tube of Different Diameters	27
6.3. Boiling at Atmospheric and Sub-atmospheric Pressure	30
7. CONCLUSION	37

REFERENCES 39
BIOGRAPHY 42
PUBLICATIONS AND PRESENTATIONS FROM THE THESIS 43

LIST OF SYMBOLS AND ABBREVIATIONS

A	:	Area
F	:	Force
q"	:	Heat flux
b	:	Growth constant
Cp	:	Specific heat capacity
ρ	:	Density
d	:	Diameter
Pr	:	Prandtl number
g	:	Gravity
h	:	Enthalpy of vaporization
σ	:	Surface tension
μ	:	Viscosity
k	:	Thermal conductivity
Re	:	Reynold number
Nu	:	Nusselt number
P	:	Pressure
V	:	Volume
K	:	Turbulent kinetic energy
T	:	Temperature
t	:	Time
s	:	Solid
α	:	Volume fraction
v	:	Velocity
η	:	Thermal diffusivity
Cw	:	Bubble waiting coefficient
N	:	Nucleation site
f	:	Frequency of bubble
evap	:	Evaporation
l	:	Liquid
tc	:	Transient conduction
ml	:	Microlayer
cl	:	Three-phase contact line
quen	:	Quenching
sl	:	Superheat liquid layer
v	:	Vapor (subscription)
nc	:	Natural convection
w	:	Wall
sup	:	super heat
sat	:	Saturation
crit	:	Critical

LIST OF FIGURES

	Page
Figure 2.1: Nukiyam's pool boiling curve for water at atmospheric pressure.	4
Figure 2.2: Diagram of bubble forces analysis on a horizontal surface (a) and vertical surface (b)	6
Figure 2.3: Illustration of bubble raising on the horizontal tube during pool boiling	6
Figure 2.4: Heat transfer mechanism on the bubble growing (a) and rising (b)	7
Figure 2.5: Detailed demonstration of microlayer and three-phase contact line	8
Figure 2.6: Transient conduction	9
Figure 3.1: Heat transfer mechanism associated with the growth of the sliding bubble	13
Figure 4.1: Geometry for the simulations	15
Figure 4.2: Mesh structure	15
Figure 4.3: Main mechanism of heat transfer	16
Figure 4.4: Boundary conditions on the geometry	21
Figure 5.1: Heat flux comparison between Saad's study and the present study	23
Figure 5.2: PBHTC comparison between Saad's study and the present study	24
Figure 6.1: Heat flux and the evolution of bubbles for the 10 mm tube at superheat temperature 6.5°C	25
Figure 6.2: Averaged heat flux and the formation of bubbles for the 0.5 mm wire from Jiaojiao's study	26
Figure 6.3: Heat flux values for different diameters based on different superheat temperatures	27
Figure 6.4: Heat flux and PBHTC values for different diameters based on 6.5°C superheat temperature	28
Figure 6.5: Bubble forming around different tube diameters (volume fraction) based on 6.5°C superheat temperature	29
Figure 6.6: Averaged heat flux, bubble diameter, and growth period based on different diameters from Jiaojiao's study	30
Figure 6.7: Heat Flux and PBHTC values on 10 mm diameter tube at atmospheric and subatmospheric pressure at superheat temperature 6.5°C	31
Figure 6.8: Heat flux values based on different pressures for water and nanofluid from XueFei Yang and Zhen-Hua Liu's study	32
Figure 6.9: The visual depiction of bubbles at different outlet pressures at 0.1 second	33
Figure 6.10: The visual depiction of bubbles at different outlet pressures at 0.2 second	33
Figure 6.11: The visual depiction of bubbles at different outlet pressures at 0.3 second	34
Figure 6.12: The visual depiction of bubbles at different outlet pressures at 0.5 second	34

Figure 6.13: The visual depiction of bubbles at different outlet pressures at 0.7 second 35
Figure 6.14: Bubble growth formation from Santra's study 36

LIST OF TABLES

		Page
Table 4.1:	Nucleate pool boiling parameters	17
Table 4.2:	Interfacial Forces	19
Table 5.3:	Properties of working fluids	22

1. INTRODUCTION

In modern times, boiling is essential for maximizing the efficiency of heat exchangers and thermal management systems. A significant amount of research is currently underway to enhance our understanding of this process. Boiling represents the thermal phenomenon wherein a liquid absorbs heat from the surface of a heating element, subsequently transitioning into the vapor phase. Due to its commendable heat transfer efficacy, this method finds widespread application across various industries, including but not limited to deployment within adsorption chillers in power generation facilities, utilization within nuclear reactors, integration within electronic systems, incorporation within boiler systems, and in diverse cooling applications. Generally, it is used where liquid's latent heat vaporization is required to transfer heat. Conventional air cooling or single-phase cooling systems lack efficiency in addressing the heat transfer needs of advanced microchips, hybrid electric vehicles, fuel cells, aircraft, spacecraft, and similar devices. However, when it comes to heat transfer in these advanced applications, two-phase cooling methods like pool boiling stand out as a superior alternative to single-phase cooling systems, providing a confident solution to thermal management challenges. [1]. In boiling, heat transfers more efficiently compared to regular convection processes. The higher heat transfer coefficients seen during boiling make it a preferred method for thermal power engineers [2].

Boiling manifests in two distinct modes: pool boiling and flow boiling. Pool boiling occurs when the boiling process takes place in a stationary or relatively quiescent liquid, where fluid movement is natural and driven by convection currents and the buoyancy of bubbles. On the other hand, flow boiling occurs when the boiling process happens within a liquid in motion, such as in channels or pipes, and the fluid is forced to move by an external source, like a pump, as it undergoes a phase-change process. These two modes are fundamental configurations in heat transfer processes in engineering domains.

Liquid density, specific heat, vapor density, latent heat of vaporization, surface tension, boiling point, and liquid thermal conductivity are among the critical liquid thermophysical properties that greatly influence boiling heat transfer. Similarly, for the surface shape, such as a straight plate or tube surface, fin type, and quantity, the

rightness of the surface strongly influences the boiling heat flux and heat transfer coefficient [3].

Considering the complexities inherent in this subject matter, numerous experiments have been conducted to comb out the boiling phenomena. These studies have collectively highlighted many factors that intricately influence the boiling heat flux. For instance, while much research has been dedicated to comprehending boiling on flat plates, equally crucial experimental inquiries elucidate the dynamics of boiling on horizontal or vertical tubes. Notably, positioning the tube itself emerges as a significant criterion impacting the boiling process. The core aim of this study is to explore nuances of heat flux and the pool boiling heat transfer coefficient (PBHTC) across a spectrum of distinct superheat temperatures ranging from 5.5°C to 7.0°C. Additionally, the study aims to express the effects resulting from alterations in tube diameter, exploring the transition from 5 mm to 20 mm diameter while maintaining a constant superheat temperature. Furthermore, an in-depth comparative analysis delineates the disparities between boiling phenomena at atmospheric and sub-atmospheric pressures set at 47 kPa, 20 kPa, 7.3 kPa, and 2 kPa.

This comprehensive investigation includes detailed scan bubble behavior dynamics, encompassing critical aspects such as the mechanism behind bubble departure and the formation of growing bubbles. In this study, ANSYS Fluent software, known for its advanced features, is used carefully to understand and explain the complex dynamics involved. Moreover, the selection of the Euler-Euler model over the Volume of Fluid (VOF) method is predicated upon its proven ability to offer superior accuracy and granularity in modeling these complex phenomena.

The findings show that the heat flux on the tube decreases with an increase in tube diameter. Another observed outcome is reduced heat transfer flux when boiling occurs under sub-atmospheric pressure conditions.

2. POOL BOILING

Pool boiling occurs when a fluid, without forced mass velocity, occurs on a heating surface at a temperature higher than the fluid's saturation temperature. Due to the elevated surface temperature surpassing that of the fluid, the local fluid temperature near the surface exceeds its saturation point. Consequently, molecules within this vicinity transition into the vapor phase, instigating the boiling process. At first, bubbles of vapor start appearing on the solid surface. Then, as more of these bubbles join and get more prominent by changing from liquid to vapor, they eventually break away from the surface, overcoming surface tension. While the fluid changes phases throughout the boiling process, its bulk temperature remains constant.

2.1. Pool Boiling Regimes

In 1934, Nukiyama's experimental work described the fundamentals of pool boiling phenomenon. [4]. He was the first scientist to introduce different steps of pool boiling based on superheat temperatures, as seen in **Figure 2.1**. A metal wire is used inside a water tank at 100 °C to check the heat flux on the wire. The result of his experiment is that the relation between the degree of superheating (T_{sup} - temperature difference between wall temperature and liquid saturation temperature) and heat flux is not monotonous. The formation of bubbles changes with superheat temperature, and the required superheat temperature is around 5°C for bubbles to occur. Outside the nucleate pool boiling heat transfer region, the critical heat flux phenomenon triggers a sudden drop in the heat transfer coefficient, leading to a sharp increase in surface temperature, known as burn-out. [5].

2.1.1. Natural Convection Pool Boiling

In the natural convection boiling region, heat transfer between the surface and fluid happens due to natural or free convection. Variations in density primarily drive fluid movement in this area. Observations indicated that the inception of bubbles was not evident until the degree of superheat reached around the onset of nucleate boiling, which is around 5°C.

In natural convection boiling, the hydrostatic pressure of the fluid at the surface prevents bubble formation.

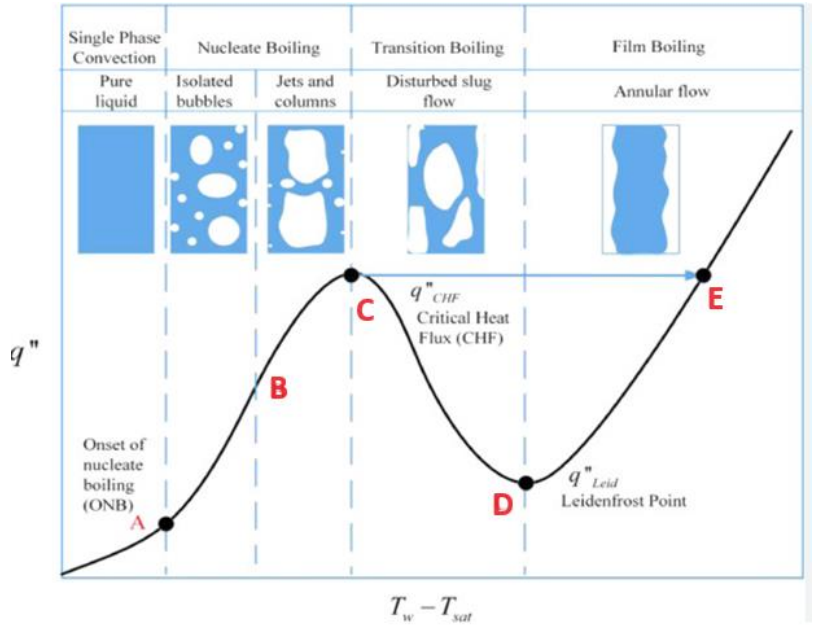

Figure 2.1: Nukiyam's pool boiling curve for water at atmospheric pressure **[4]**.

2.1.2. Nucleate Pool Boiling

Nucleate boiling, recognized as a highly efficient method for heat transfer, stands as a widely investigated phenomenon in science and engineering. In instances of lower heat flux, characterized by the isolated growth of bubbles. Point A in **Figure 2.1** shows the beginning of nucleation. Nucleate pool boiling can be broken down into two stages: partial nucleate and fully developed nucleate boiling. In the regime between A and B bubble detaches from the surface. It may either dissipate within the fluid by condensing, reliant upon the vapor energy within the bubble or ascend to reach the top of the liquid surface. In the region between points B-C on the boiling curve, bubbles combine and grow larger before separating from the surface. They raise as vapor jets or columns towards the surface. As the surface temperature rises, more vapor jets appear, resulting in continuous vapor columns on the surface. At point B, a significant event occurs: the heat transfer coefficient reaches its peak before declining. However, despite this decrease, the heat flux continues to rise due to the heat transfer rate being linked to both the heat transfer coefficient and superheat temperature. In equation 1.1,

T_w represents the temperature of the tube wall, T_{sat} denotes the saturation temperature of the fluid, and h represents the enthalpy.

$$q'' = h\,[T_w - T_{sat}] \tag{1.1}$$

2.1.3. Transition Pool Boiling

The nucleate boiling heat flux cannot be endlessly increased, reaching a point known as the "critical heat flux" (CHF), which is shown as point C in **Figure 2.1** Between points C-D, bubble formation occurs rapidly, leading to the development of a vapor film on the surface. This vapor film has a lower thermal conductivity of vapor compared to that of the liquid, and it acts as thermal insulation. It causes a reduction in the heat flux and the lowest heat flux observed in this regime.

2.1.4. Film Pool Boiling

The heat flux forms a vapor film that completely covers the surface during film boiling. His results in a notable decrease in the boiling convection coefficient. Bubbles that form struggle to escape promptly. Additionally, when the temperature rises further, more bubbles emerge. However, as the temperature keeps increasing, an excess of bubbles forms, exceeding the efficient removal capacity. These bubbles grow more extensive and gather, creating patches of steam film on some regions of the heat transfer surface. Beyond the Leidenfrost point, the surface becomes entirely enveloped by a continuous vapor film, eliminating any contact along the boundary of the liquid and the surface. Under these circumstances, heat transfer occurs primarily through radiation and conduction to the vapor medium.

2.2. Forces on Bubble and Behavior of Bubble

In pool boiling, the bubble occurs in a repeating action; however, the action is much more complex since various forces and different types of heat transfer mechanisms are involved in the process. **Figure 2.2** illustrates the five fundamental forces exerted on bubbles throughout the pool boiling process, a widely acknowledged phenomenon. Surface tension (F_s), buoyancy force (F_b), drag force (F_d), inertia force (F_i), and pressure force (F_p) affect bubbles [6].

The process starts with a small nucleate, where tiny bubbles form at nucleation sites on the heated surface. Defects, cavities, or roughness on the surface can be caused among sites where vapor pockets occur. Nucleate follows with its growth. When the upward forces like buoyancy force overcome the force dragging, the bubble detaches from the heated surface and lifts inside the bulk liquid. Buoyancy force works against surface tension, trying to detach the bubbles and allow them to rise through the liquid.

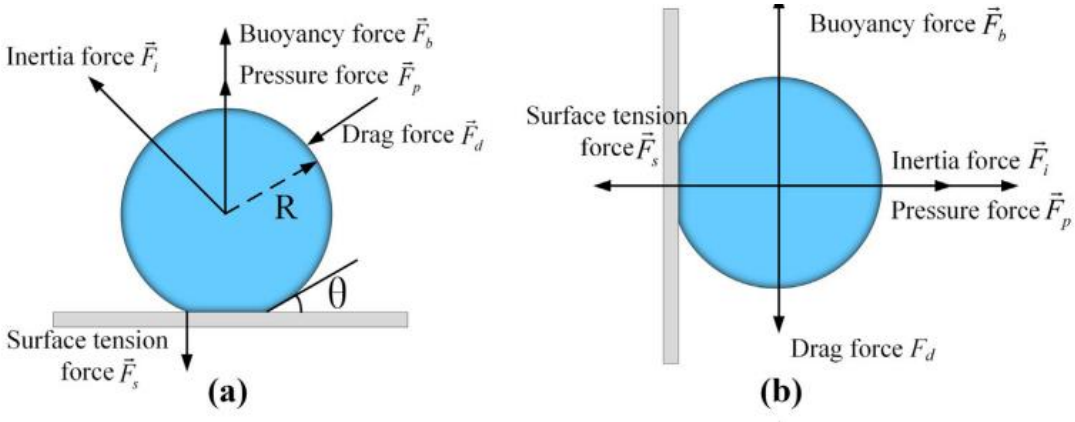

Figure 2.2: Diagram of bubble forces analysis on horizontal surface(a) and vertical surface(b) **[6]**

The behavior of bubbles on a horizontal tube is different than on a flat surface. Around a horizontal tube, nucleation sites are intensived on the bottom side of the tube due to gravity. When bubbles rise, they follow a convective path around a tube, and this motion of liquid moves to bubbles on top of the tube, contributing to an increased concentration of bubbles in the upper section of the tube [7]. **Figure 2.3** illustrates how bubbles evolve around the tube.

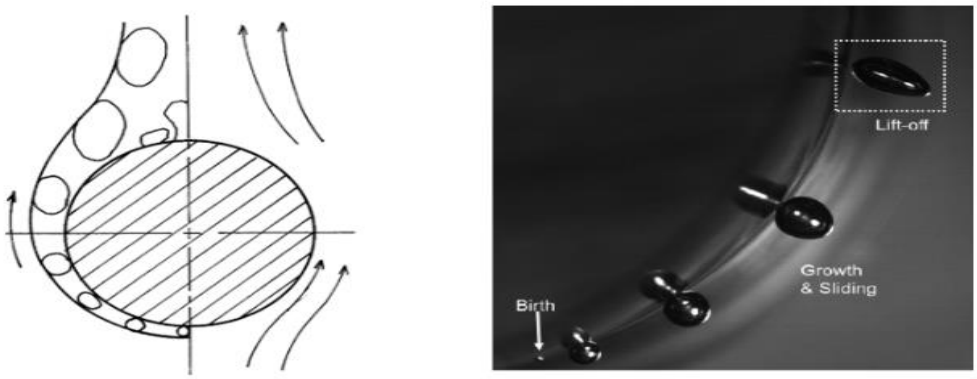

Figure 2.3: Illustration of bubble raising on the horizontal tube during pool boiling **[7-8]**

2.3. Heat Transfer Mechanism

Many researchers have investigated the heat transfer mechanism, showing numerous heat fluxes affecting bubbles from nucleate to quenching. Heat transfer mechanisms during the bubble departure process are illustrated in **Figure 2.4**.

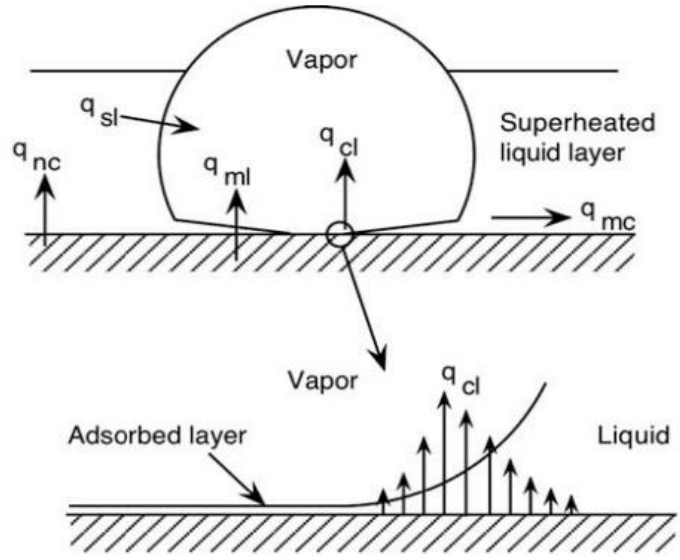

a)

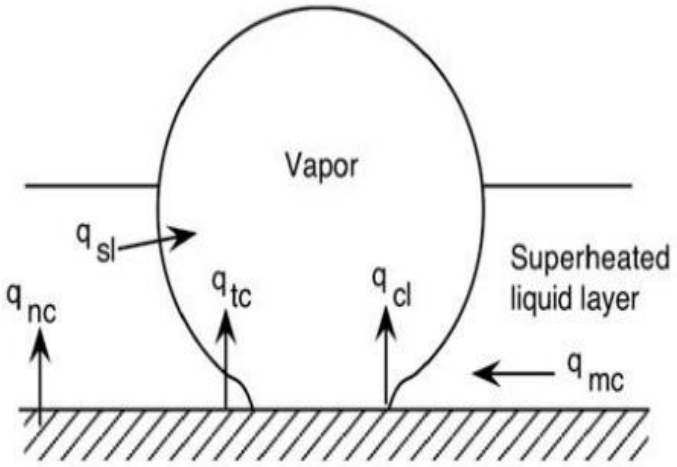

b)

Figure 2.4: Heat transfer mechanism on the bubble growing (a) and rising (b) **[9]**

The microlayer refers to a thin liquid film that becomes trapped beneath a vapor bubble near a three-phase contact line. The evaporation of this liquid facilitates bubble growth (q_{ml}). The energy needed for evaporating this liquid originates from the energy stored

in the superheated wall [9]. The microlayer region experiences extraordinarily high heat fluxes due to its low thermal resistance, which is directly related to the thickness of the liquid layer [10]. Evaporation occurs within the thermal boundary layer surrounding the bubble cap (q_{sl}).

Suddenly, after the creation of the dry spot resulting from the microlayer's partial dry-out, another evaporation mechanism takes place at the three-phase contact line(q_{cl}), further supporting the expansion of the bubble. When a dry area appears on the surface because the microlayer partly dries out while a bubble grows, this dry area gets wet again with liquid when the bubble moves away. Heat is transferred at the spot where the liquid, solid, and vapor meet, but this heat transfer is predicted to be less than during bubble growth. This is because the angle at which the liquid advances is steeper than when it retreats, causing a thicker layer of liquid on the surface [9].

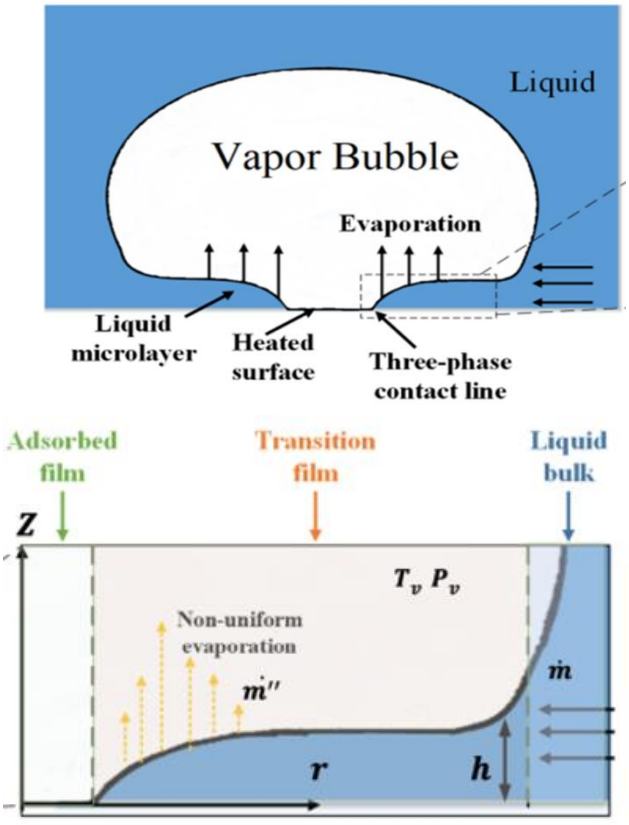

Figure 2.5: Detailed demonstration of microlayer and three-phase contact line **[10]**

As can be seen from **Figure 2.6**, the surface where a dry area (dry patch) exists suddenly starts to cover this dry area again (rewetting). As the liquid spreads and covers this dry patch, heat from the surface transfers into the liquid. This transfer of

heat from the surface into the advancing liquid as it covers the dry area is referred to as transient conduction (q_{tc}) into the advancing liquid.

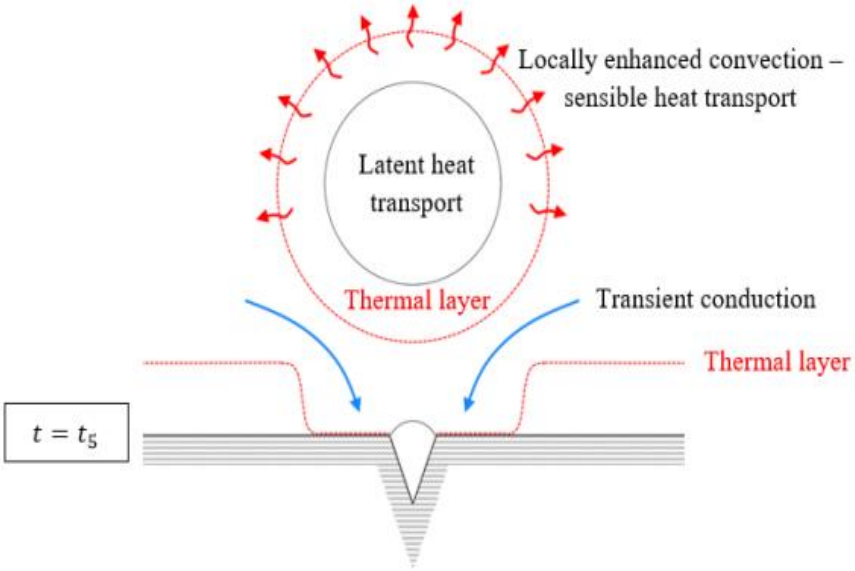

Figure 2.6: Transient conduction **[11]**

3. LITERATURE REVIEW

3.1. Experimental and Numerical Studies

Boiling heat transfer stands out as an exceptionally efficient heat exchange mode, finding widespread applications across diverse technological and industrial domains. Its utilization extends to heat-exchange systems, energy conversion processes, and the essential cooling of high-power electronics and nuclear reactors. This inherent efficiency in heat transfer makes boiling a cornerstone in the design and operation of various engineering systems. Gorgy and Eckels [12] looked at the local heat transfer coefficient for pool boiling of R-134a on both smooth and enhanced tubes. They used warm water flowing inside the tubes to induce pool boiling. On the enhanced tube, they observed two distinct regions in the pool boiling curve. In the first region, the heat transfer coefficient increased significantly with the heat flux. However, the heat transfer coefficient remained approximately constant in the second region regardless of the heat flux. As a result, both regions of the pool boiling curve could be accurately represented using an appropriate power law model.

In another study, Chien and Webb [13] examined how the shape of surfaces with "tunnels" affects the boiling heat transfer coefficient. They tested this on a horizontal tube with a diameter of 19.1 mm and different pore sizes and pitches. They used refrigerants like R11 and R123 at 26.7 °C with heat fluxes ranging from 2 to 70 kW/m². The findings revealed that the boiling heat transfer coefficient increased when tunnel height and tunnel pitch decreased. Additionally, they discovered that sharp corners in the tunnels led to more significant enhancement in heat transfer rates.

Ribatski [14] measured the local heat transfer coefficient in a vertical array of horizontal pipes under flooded conditions. No matter how the tubes are arranged, they noticed that there's a point where the local heat transfer coefficient reaches a maximum along the vertical direction. After this point, the heat transfer rate decreases and doesn't increase much further.

Gorenflo et al. [15] conducted experiments on nucleate boiling over a horizontal tube using methane. They gathered experimental data covering a range of pressures from atmospheric pressure to critical pressure.

Yagov et al. [16] conducted an early experiment on sub-atmospheric pool boiling. They explored boiling water, ethyl alcohol, and NaCl solutions under low pressures. The experiment revealed prolonged periods of vapor formation, the presence of millimeters-sized bubbles, and significant disturbances in the liquid. Their findings indicated that as the pressure decreased, both the time it takes for bubbles to grow and the radius at which they depart increased.

Abadi et al. [17] conducted a Fluent simulation to investigate boiling in a system comprising two inclined and electrically heated circular tubes. A specific methodology was employed to characterize the flow of both liquid and vapor phases, supplemented by a model from Rensselaer Polytechnic Institute to elucidate heat and mass transfer phenomena during boiling. Their findings revealed that water exhibited the highest heat transfer coefficient across all simulated scenarios, while FC-72 demonstrated the lowest. Furthermore, the study indicated that an increase in the inclination angle of the heated tubes led to a reduction in the pool boiling heat transfer intensity. Additionally, it was noted that activation of the lower tube resulted in increased pool boiling heat transfer in the upper tube.

3.2. Heat Flux Correlations in Literature

Many early models investigated by scientists are based on the primary mechanism for heat transfer by driven or micro-convection of bubbles; however, these models did not include phase change and were investigated based on single-phase convection. Some of those correlations are listed below.

Rohsenow [18] established a correlation that uses the equation for forced convection heat transfer.

$$Cp_l \frac{T_w - T_{sat}}{h_{fg}} = C_{sf} \frac{q''}{\mu_l h_{fg}} \left[\left(\frac{\sigma}{g(\rho_l - \rho_v)} \right)^{0.5} \right]^{0.33} Pr \qquad (3.1)$$

C_{sf} represents a coefficient determined by the specific surface and fluid combination involved.

Forster and Zuber [19] developed a correlation for nucleate boiling heat flux, which considers surface effects.

$$\frac{q''Cp_l\rho_l\left(\frac{\pi}{\alpha_l}\right)^{0.5}}{k_l h_{fg}\rho_v}\left(\frac{2\sigma}{\Delta P_{sat}}\right)^{0.5}\left(\frac{\rho_l}{\Delta P_{sat}}\right)^{0.25}=0.0015Re_v^{0.62}Pr_l^{1/3} \quad (3.2)$$

Borishansky's [20] correlation defines heat flux based on reduced pressure function, as seen in equation 3.3 below.

$$q''=(A^*)^{3.33}(T_w-T_{sat})^{3.33}[F(P_r)]^{3.33} \quad (3.3)$$

$$P_r=P/P_{crit} \quad (3.4)$$

$$A^*=0.1011P_{crit}^{0.69} \quad (3.5)$$

$$(P_r)=1.8P_r^{0.17}+4P_r^{1.2}+10P_r^{10} \quad (3.6)$$

The heat partitioning model is a highly accepted method for understanding how heat transfer occurs during boiling. It's a mechanistic model that accurately represents the creation of vapor bubbles and real-world phenomena. Researchers find it valuable because it can be easily applied, initially introduced by Kurul and Podowski [21]. The heat partitioning model, also known as the RPI model, which is used in this study as well, was first created to understand how heat moves during boiling on a flat surface. This model explains heat transfer by considering three main ways heat moves between the surface and the liquid: evaporation, transient conduction, and single-phase convection.

$$q''_{total}=q''_{evap}+q''_{tc}+q''_{nc} \quad (3.7)$$

Equation 3.5 explains the evaporation heat flux suggested by Yoo et al. [22], and it is based on the time of bubble sliding.

$$q''_{evap}=q''_{ml}+q''_{sl} \quad (3.8)$$

i. Microlayer evaporation:

$$q''_{ml}=\gamma Pr^{-0.5}[\rho_l Cp_l(T_w-T_{sat})]\eta_l^{0.5}t_{sliding}^{-0.5} \quad (3.9)$$

Unal [23] determined γ coefficient as below,

$$\gamma=\frac{k_s\rho_s c_s}{k_l\rho_l Cp_l}^{0.5} \tag{3.10}$$

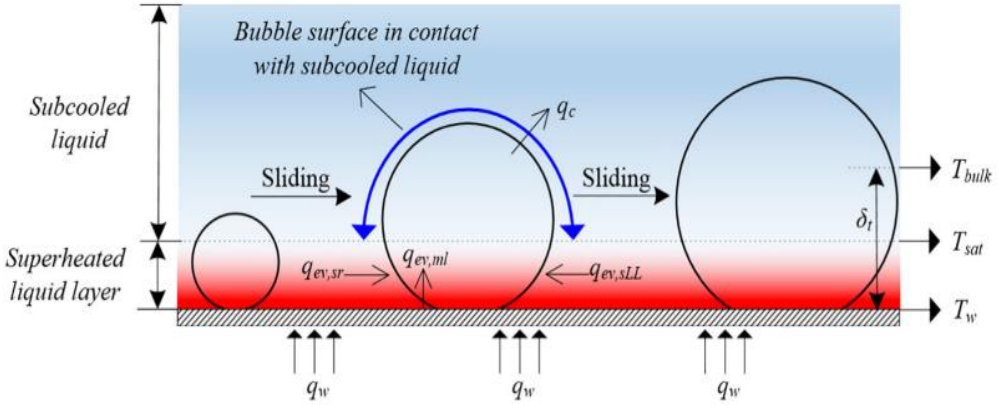

Figure 3.1 Heat transfer mechanism with the growth of sliding bubble **[22]**

ii. Superheated liquid layer evaporation:

$$q''_{sl}=\frac{bk_l[Tw-Tsat]}{\pi\eta_l t_{sliding}^{0.5}} \tag{3.11}$$

The formula of time-averaged transient conduction is expressed as below [24]

$$\frac{1}{t^*}\int_0^{t^*}\frac{k_l(T_w-T_l)}{\sqrt{\pi\alpha_l t}}dt \tag{3.12}$$

Another part of total heat flux based on Kurul and Podowski's study is natural convection, and it is explained by Joen et al. [25] by an experiment which is one by using a horizontal tube.

$$q''_{nc}=0.0117Re_D^{0.514} \tag{3.13}$$

4. NUMERICAL MODELING

4.1. Problem Definition

As observed in the literature review, investigating heat flux and heat transfer coefficients in the phenomenon of boiling is quite challenging due to their dependence on numerous parameters. Similarly, although heat flux has been examined on horizontal tubes in the literature, it has typically been studied on a single diameter or generally under atmospheric pressure conditions. In this study, the initial part involves an examination of heat flux and pool boiling heat transfer coefficients, focusing on varying tube diameters (5 mm, 10 mm, 15 mm, 20 mm). The second aspect delves into investigating alterations in heat flux and heat transfer coefficients when transitioning from atmospheric pressure to sub-atmospheric (101 kPa, 47 kPa, 20 kPa, 7.4 and 2.3 kPa) pressure conditions. Moreover, bubble behavior was investigated based on different diameters and varying pressure values.

4.2. Geometry and Mesh

This investigation entails numerical simulations of pool boiling heat transfer phenomena occurring from horizontal copper tubes. The computational domain's physical geometries were established in two dimensions utilizing the Creo PTC, and the structural grids were generated through the meshing tool within the Ansys software suite.

Before simulating the studies explained in the problem definition, Mohammad Saad's [26] study was verified, and the same results were obtained. **Figure 4.1** shows the simulated geometry.

The dimensions of the plane under consideration have been specified as 150 mm in length and 100 mm in height. In conformity with the parameters established by Saad's study for validation, the diameter of the heated tube is maintained at 10 mm, and the material is Copper. Additionally, simulations have been conducted for alternative tube diameters, namely 5 mm, 15 mm, and 20 mm.

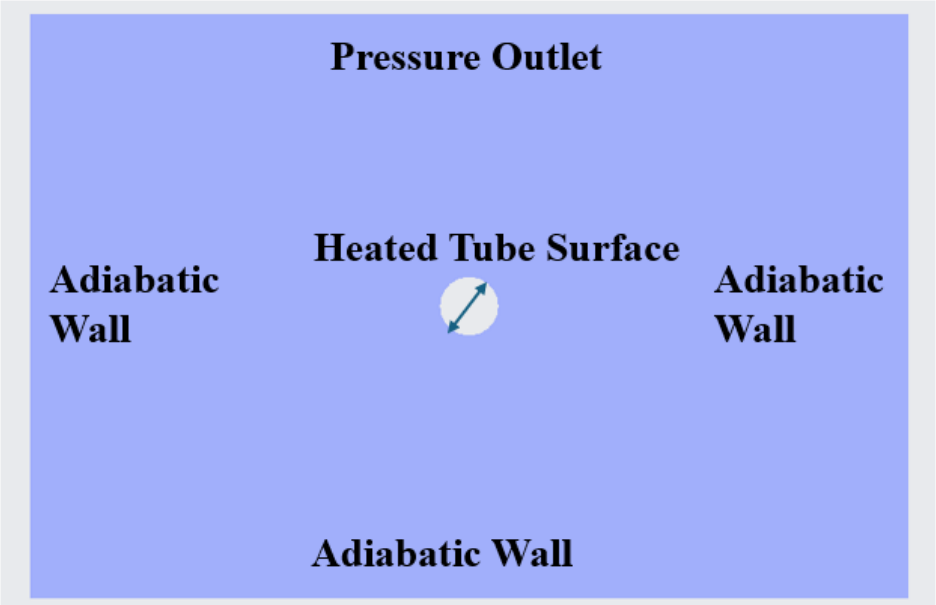

Figure 4.1 Geometry for the simulations

The mesh generation tool integrated into the ANSYS software suite was employed to discretize the geometry, utilizing 15,024 elements within the computational mesh. This numerical configuration aligns with the specifications outlined in Saad's study for congruence in the investigative approach.

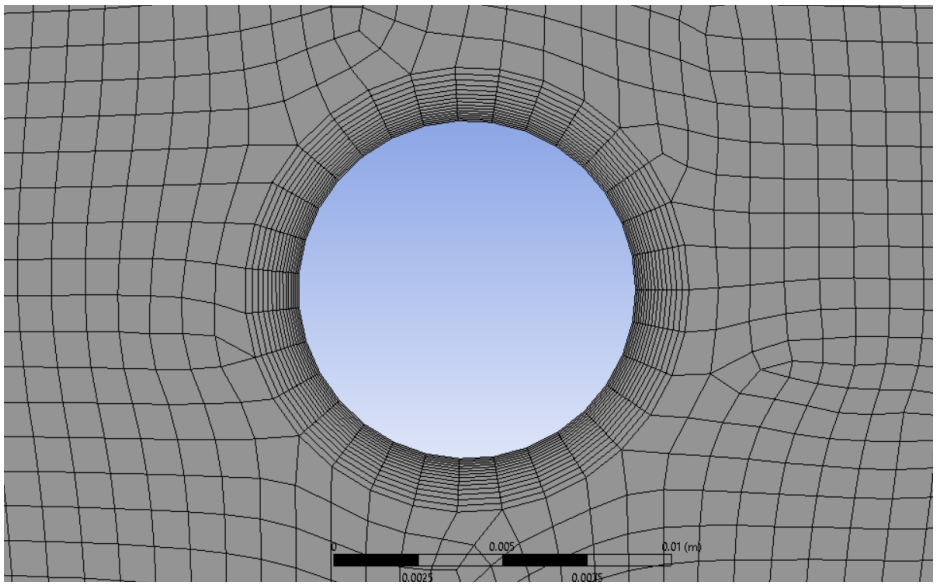

Figure 4.2 Mesh structure

4.3. Governing Equations

As discussed in the literature section, the Rensselaer Polytechnic Institute (RPI) model is employed to forecast heat and mass transfer in nucleate pool boiling of pure liquids. The heat flux from the heating wall is divided into liquid convection, quenching, and evaporation components, as illustrated in **Figure 5.3**.

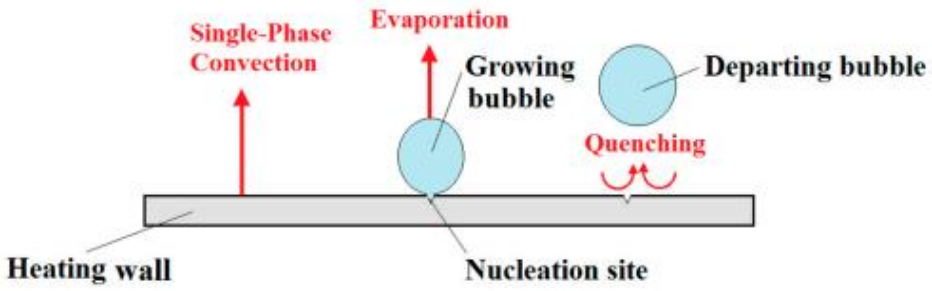

Figure 4.3 Main mechanism of heat transfer **[27]**

$$q''_{conv} = h_{single}(T_w - T_l)(1 - A_{bubbles}) \quad (4.1)$$

$$q''_{quen} = C_w \frac{2k_l}{\sqrt{\pi\lambda t}} (T_w - T_l)A_{bubble} \quad (4.2)$$

$$q''_{evap} = V_d N \rho_v h_{fg} f \quad (4.3)$$

The equations in the heat flux partitioning model, which account for three heat flux mechanisms, require specific boiling parameters to predict how nucleate boiling happens accurately. To fill in these parameters, researchers have developed many correlations found in the literature. The correlations referenced below have been employed within the scope of our study.

Table 4.1: Nucleate pool boiling parameters [26]

Nucleate Boiling Parameters	References	Correlations	
Nucleation sites density	Lemmert and Chawla	$Na=C^n(T_w-T_{sat})^n$ n=1.805 and C=210	(4.4)
Bubble departure diameter	Tolubinski and Kostanchuk	$d=\min(0.0014,0.0006e^{(Tw-Tsat)/0.45})$	(4.5)
Bubble departure frequency	Cole	$f=\sqrt{\frac{4g(\rho_l-\rho_v)}{3\rho_l d_{bubble}}}$	(4.6)
Area of Influence	Del Valle and Kennings	$A_{bubble}=\min(1,U\frac{Na\pi d^2_{bubble}}{4})$ U is the emperical constant and set to 4	(4.7)

In the Eulerian multiphase model, which is widely used to simulate two-phase flows, the behavior of the fluid is described by dividing it into distinct phases. In this model, the continuous phase represents the primary fluid medium, typically the liquid component, which fills most of the domain. Conversely, the dispersed phase consists of vapor bubbles or any other secondary fluid phase that exists within the continuous medium. This approach allows for the independent treatment of each phase, enabling the modeling of complex interactions such as phase change phenomena like boiling or condensation. Consequently, this model incorporates diverse forms of coupling interactions between these phases. Notably, the pressure is shared uniformly among all existing phases, while individual solutions for continuity, momentum, and energy equations are concurrently determined for each distinct phase within this modeling framework [17].

Continuity equation:

$$\frac{\partial(\rho_k\alpha_k)}{\partial t}+\nabla(\rho_k\alpha_k v_k)=\dot{m}_{kp}-\dot{m}_{pk} \quad (4.8)$$

Momentum Equation:

$$\frac{\partial(\rho_k \alpha_k v_k)}{\partial t} + \nabla(p_k a_k \vec{v}_k \vec{v}_k) = -\alpha_k \nabla P + \rho_k \alpha_k \vec{g} + \nabla \tau_k + (\dot{m}_{kp} v_k - \dot{m}_{pk} \vec{v}_k) + S_{1k} \quad (4.9)$$

Energy Equation:

$$\frac{\partial(\rho_k \alpha_k E_k)}{\partial t} + \nabla(\rho_k \alpha_k \vec{v}_k E_k) = \alpha_k \frac{\partial P}{\partial t} + \nabla q_k + Q_{exchange,pk} + (\dot{m}_{kp} E_k - \dot{m}_{pk} E_{p)} + S_{2k} \quad (4.10)$$

Where the subscript indicating k represents the kth phase, k = l for the liquid phase, and k = v for the vapor phase. m_{kp} represents the rate of interfacial mass transfer occurring within the liquid phase adjacent to the surface heater. This parameter accounts for the exchange of mass between the liquid and vapor phases at the interface. In contrast, within the bulk liquid, where pool boiling originates at the saturation temperature, this interfacial mass transfer is negligible and thus assumed to be zero. Additionally, S_{1k} and S_{2k} denote the inter-phase momentum transfer term, the inter-phase energy transfer term, and direct heat transfer to phase "k".

$$Q_{exchange,pk} = h_{interfacial} A_{interfacial} (T_p - T_k) \quad (4.11)$$

In the current simulations, the resolution of the governing equations describing phase interaction involving interfacial momentum, heat, and mass transfer is undertaken. Initially, in the viscous model, two distinct flow regimes, namely laminar and turbulent models, are considered. Given the chaotic nature of vapor bubbles and their associated dynamics, a robust model addressing this complexity is chosen. The realizable two-equation K − ε model is opted for, as it is a recommended approach owing to its effectiveness.[26]

The dynamic interplay between the liquid and vapor phases can lead to the emergence of several distinct forces that influence the behavior of the system. These forces include the viscous drag force, which arises from the resistance encountered by the fluid as it moves past surfaces; the lift force, generated by the pressure gradients within the fluid; the wall lubrication force, which facilitates smooth motion near solid boundaries, and the turbulent dispersion force, resulting from the chaotic movement of fluid particles in turbulent flows. These forces collectively contribute to the complex dynamics observed in multiphase systems undergoing boiling processes. In the present

study, intricate correlations are employed within the ANSYS Fluent software framework to address and resolve phase interactions.

$$S_{1k}=F_{drag}+F_{lift}+F_{dispersion}+F_{wall\ lub} \quad (4.12)$$

Table 4.2: Interfacial Forces [26]

Boiling Parameters	**References**	**Correlations**
Drag Force	Schiller-Naumann	$F_{drag}=\frac{C_D Re}{24}$ (4.13) $C_D=\frac{24(1+0.15Re^{0.687})}{Re}$ (Re<1000) (4.14) $C_D=0.44$ (Re>1000) (4.15) $Re_l=\frac{\rho\lvert\vec{v}_v-\vec{v}_l\rvert}{\mu_l}$ (4.16)
Lift Force	Tomiyama	$F_{lift}=-C_L\alpha_v\rho_l(\vec{v}_l\vec{v}_g)\nabla\vec{v}_l$ (4.17)
Turbulent Dispersion Force	Lopez-de-Bertodano	$F_{disersion}=C_{TD}\rho_l K_l\nabla\alpha_v$ (4.18) C_{TD} is equal to 1 by default $\nabla\alpha_v$ is the gradient of the vapor phase volume fraction
Wall Lubrication Force	Antal et al.	$F=C_{WL}\rho_l\alpha_v\lvert\vec{v}_l\vec{v}_v\rvert^2 n_w$ (4.19) C_{W1} = -0.01, C_{W2} = 0.05 are non-dimensional coefficients n_w is wall lubrication coefficient
Heat Exchange Coefficient	Ranz-Marshall	$Nu_v=2+0.6Pr_l^{0.33}Re_v^{0.5}$ (4.20) $h_{interfacial}=\frac{k_l Nu_v}{d_{bubble}}$ (4.21)

The non-dimensional coefficients C_D, C_L, and C_{TD} have been established as default values within the ANSYS Fluent software framework for our computational analysis.

4.4. Numerical Method

This study uses the phase-coupled SIMPLE (PC-SIMPLE) method to connect pressure and velocity in the fluid flow. This method solves velocity for each phase separately while adjusting pressure to ensure total continuity. The coefficients for pressure corrections from momentum equations for each phase are determined. A second-order upwind scheme calculates momentum, turbulent kinetic energy, and turbulent dissipation rate. A first-order upwind scheme is used for the energy equation. It computed gradients for all flow variables using the least-square cell-based method. Additionally, to handle the vapor volume fraction equation, the first-order upwind scheme is selected—this balanced stability with accuracy for tracking interfaces in multiphase flows, as recommended by previous studies. Residuals are fixed to 10^4 to cover all equations.

- Simulations involve transient and turbulent fluid flow.
- It is considered the thermodynamic properties of vapor and water do not change during the simulation.
- A time step size of 0.001 seconds was selected for the present work. Additionally, the maximum number of iterations per time step was constrained within the range of 100 to 150.

4.5. Boundary Conditions

The following boundary conditions have been applied for the simulations.

- It is assumed the surface temperature of the horizontal tube is not changing, and temperatures 105.5, 106.0, 106.5, and 107.0 degrees have been applied successively.
- At the adiabatic walls of the boiling chamber, the heat flux is zero.
- The pressures at the top of the boiling chamber are assumed to be 101 kPa, 47 kPa, 20 kPa, 7.4 kPa, and 2.3 kPa, **Figure 4.4**.

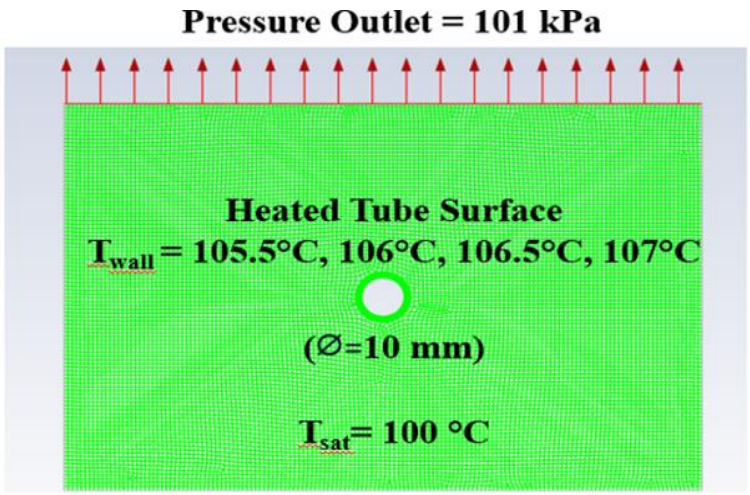

a)

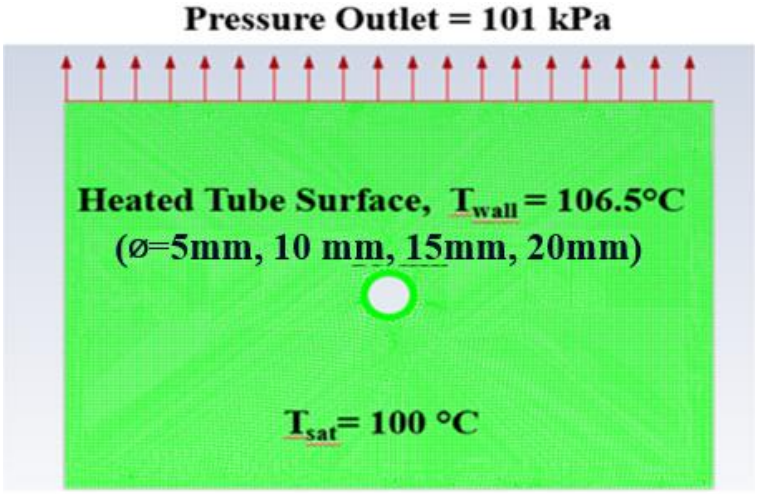

b)

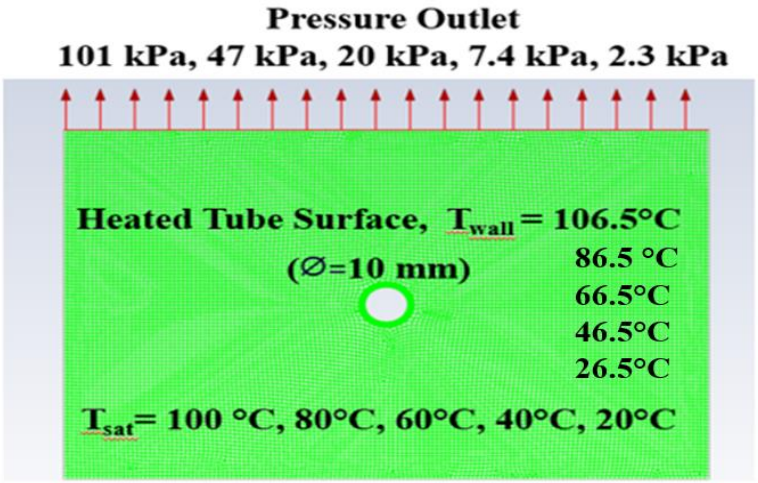

c)

Figure 4.4 Boundary conditions on the geometry. Simulation 1 (a), simulation 2 (b), simulation 3 (c)

In **Figure 4.4**, the boundary conditions are illustrated on the geometry used for simulation 1 validation, the same as Saad's [26] study. Simulations 2 and 3 were conducted within the scope of this thesis.

4.6. Properties of Working Fluids

The thermophysical properties of pure water and vapor at the different saturation pressure temperatures are presented in **Table 4.3**.

Table 5.3: Properties of working fluids

Fluid	**T_{sat} °C**	**P_{sat} kPa**	**ρ kg/m³**	**Cp Jkg/K**	**k W/mK**	**μ Pas**	**σ N/m**
	100	101	957	4216	0.68	$0.28x10^{-3}$	0.061
	80	47	971	4197	0.67	$0.35x10^{-3}$	0.065
Water	60	20	983	4185	0.65	$0.46x10^{-3}$	0.074
	40	7.4	992	4179	0.63	$0.65x10^{-3}$	0.076
	20	2.3	998	4182	0.60	$1.00x10^{-3}$	0.080
	100	101	0.60	2029	0.020	$1.22x10^{-5}$	-
	80	47	0.29	1962	0.023	$1.16x10^{-5}$	-
Vapor	60	20	0.13	1916	0.021	$1.09x10^{-5}$	-
	40	7.4	0.05	1885	0.020	$1.03x10^{-5}$	-
	20	2.3	0.02	1867	0.018	$0.97x10^{-5}$	-

5. MODEL VALIDATION

Saad's experimental investigation of boiling, which encompassed both water and nano-fluids within channels, was considered for model validation. Saad endeavored to validate his experimental findings through computational fluid dynamics (CFD) simulations. The experiment was conducted with a diameter of 10 mm and varying degrees of superheat at atmospheric pressure.

During the validation phase of this thesis, attempts were made to reproduce identical results to those obtained by Saad, subsequently leading to the validation of the model. Following the validation of the model, CFD simulations were conducted under different diameters and pressures. **Figures 5.1 and 5.2** display heat flux and PBHTC results in comparison between Saad's [26] study and the present study.

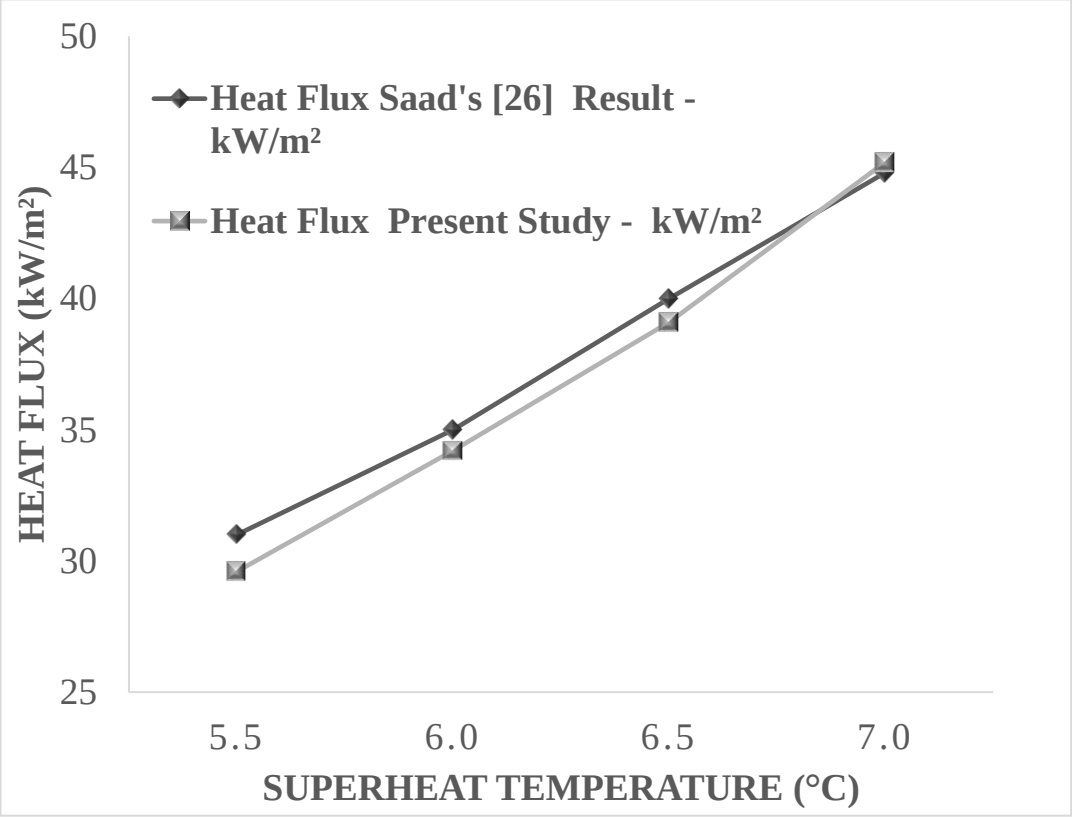

Figure 5.1: Heat flux comparison between Saad's [26] study and the present study

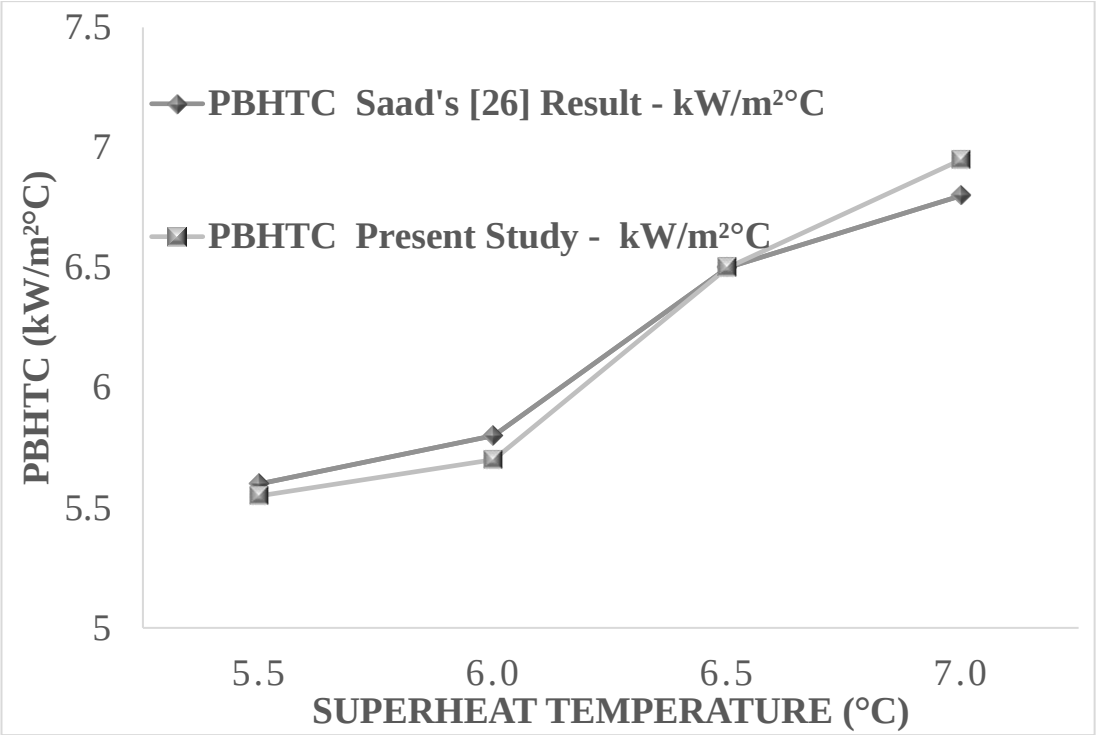

Figure 5.2: PBHTC comparison between Saad's [26] study and the present study

As evidenced by the graphs, the study conducted in this research yielded similar results to Saad's work, with a maximum difference of only 5% observed at a mere 5.5°C for heat flux and 7.0°C for PBHTC. Consequently, the model was deemed accurate, and the focus shifted toward the primary objective of investigating heat flux variations dependent on different diameters and pressure values.

6. RESULTS AND DISCUSSION

6.1. Bubble Forming on Horizontal Tube

As mentioned in the preceding sections, it would be beneficial to observe how bubble formation and heat flux evolve over time before delving into simulations based on different diameters and pressure values. This approach allows us to better understand the temporal changes in these phenomena. Additionally, cross-referencing our findings with existing literature will enhance the reliability of this CFD study.

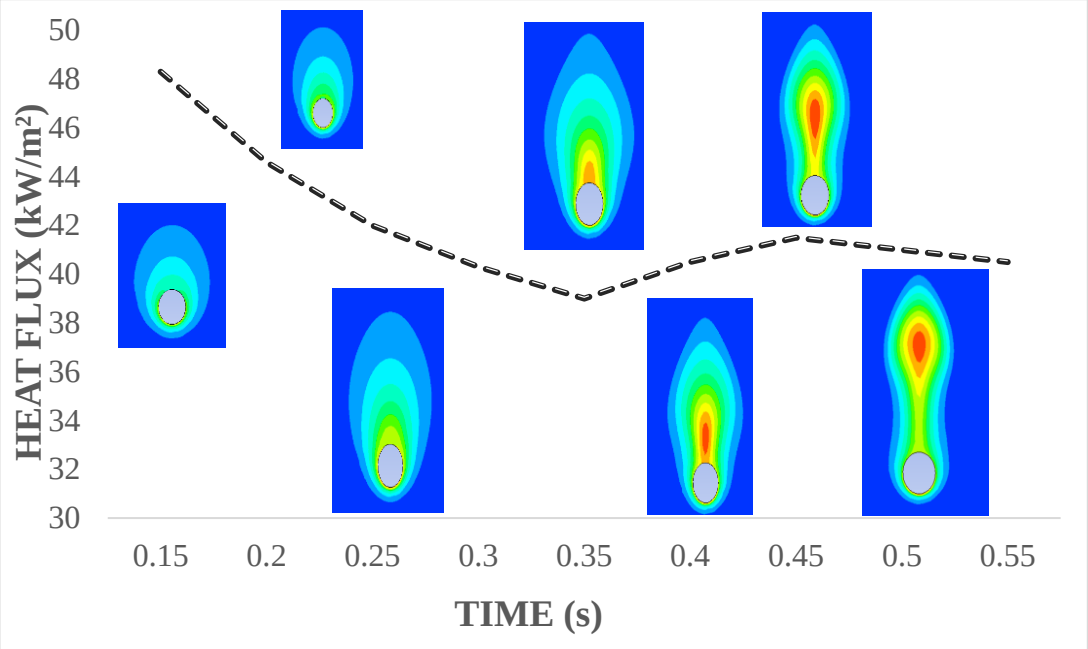

Figure 6.1: Heat flux and the evolution of bubbles for the 10 mm tube at superheat temperature 6.5°C

Figure 6.1 depicts the progression of bubble formation and the averaged heat flux during film boiling across the surface of the 10 mm tube by keeping the superheat temperature at 6.5°C. The emergence and detachment of bubbles align with the characteristic cycle of heat flux variation. As the heating surface becomes enveloped by a thick gas film, there is a subsequent decrease in the average heat flow owing to heightened thermal resistance and gas behavior as insulation. However, as gas accumulates on the upper section of the wire, facilitated by buoyancy, and begins to take on a bubble formation, the gas film covering the wire's surface thins, leading to a

gradual increase in the average heat flux until the bubble departs from the tube. Jiaojiao et al. [28] researched film boiling of hydrogen on a horizontal tube and utilized various tube diameters. In **Figure 6.2**, the investigation of bubble formation's impact on heat flux in hydrogen film boiling by using the VOF model is depicted. This study bears clear similarities with Jiaojiao's research.

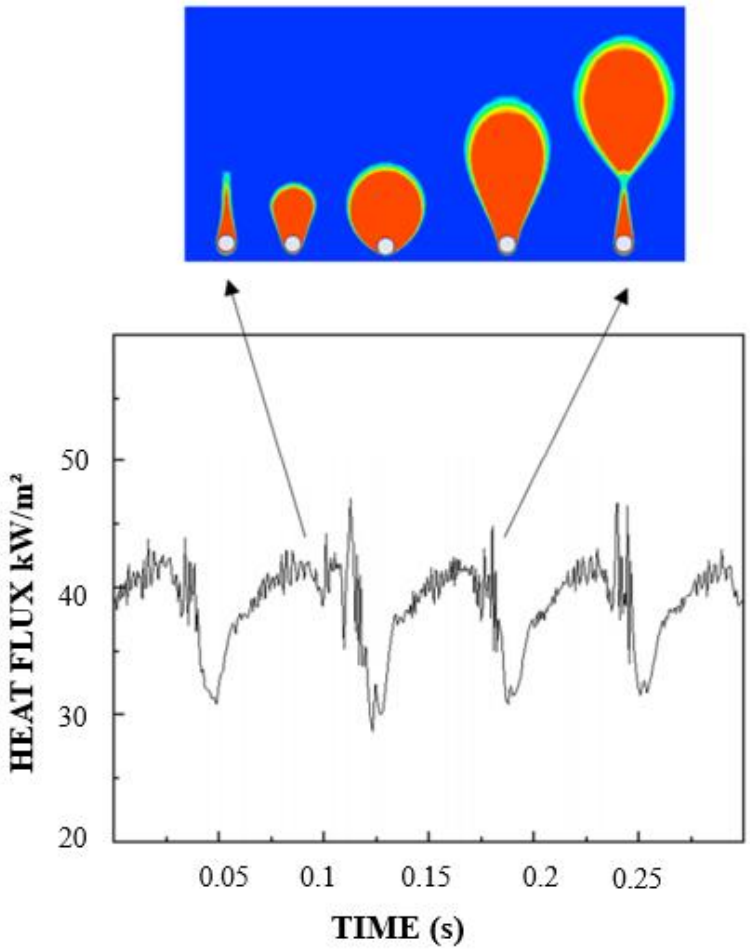

Figure 6.2: Averaged heat flux and the formation of bubbles for the 0.5 mm wire from Jiaojiao's **[28]** study.

6.2. Boiling Around Horizontal Tube of Different Diameters

The comparison of averaged heat flux among heating surfaces of four typical diameters with different superheat temperatures (5 mm, 10 mm, 15 mm, and 25 mm tubes) are presented in **Figure 6.3** and **Figure 6.4.** Notably, as the diameter increases, there is a discernible decrease in both the fluctuation amplitude and the average heat flux value. This observation underscores the influence of diameter size on heat transfer characteristics.

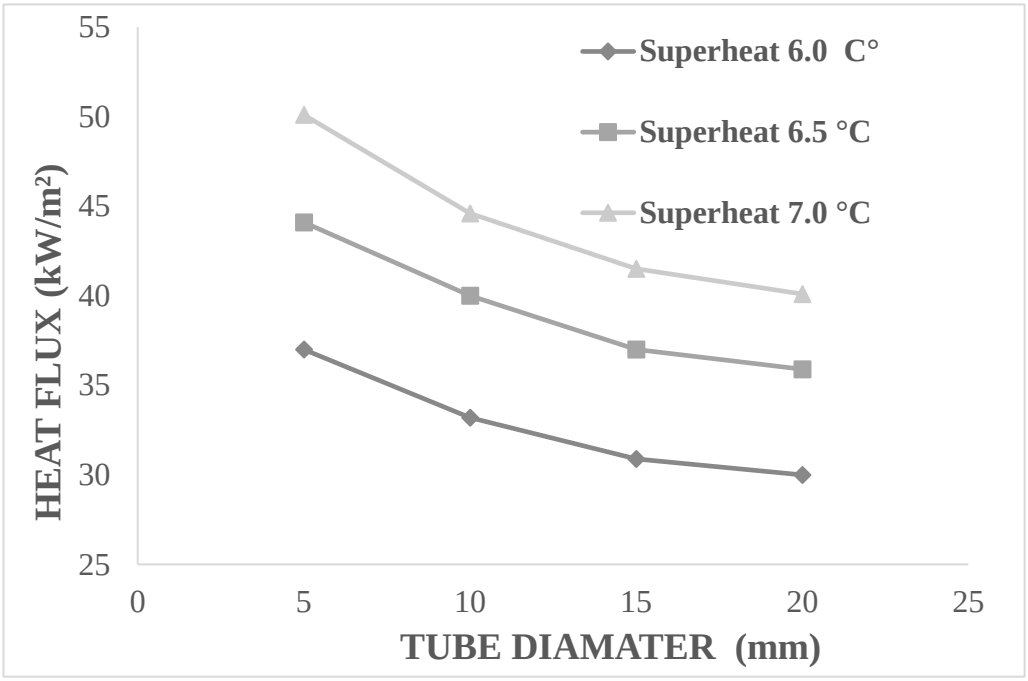

Figure 6.3: Heat flux values for different diameters based on different superheat temperatures.

Upon closer examination, it becomes apparent that while there are similarities, there are also notable differences between the heat transfer dynamics of small-diameter tube heaters and those of large-diameter tube heaters. Integrating this insight with the preceding analysis, it can be inferred that the heat transfer process on the wire surface is predominantly influenced by the evolution of individual bubbles. Conversely, on the tube surface, heat transfer is primarily impacted by the movement of multiple crescent-shaped gas structures along its surface. This distinction highlights the nuanced interplay between diameter size and heat transfer mechanisms, shedding light on the

intricate dynamics governing nucleate boiling phenomena across varying surface geometries.

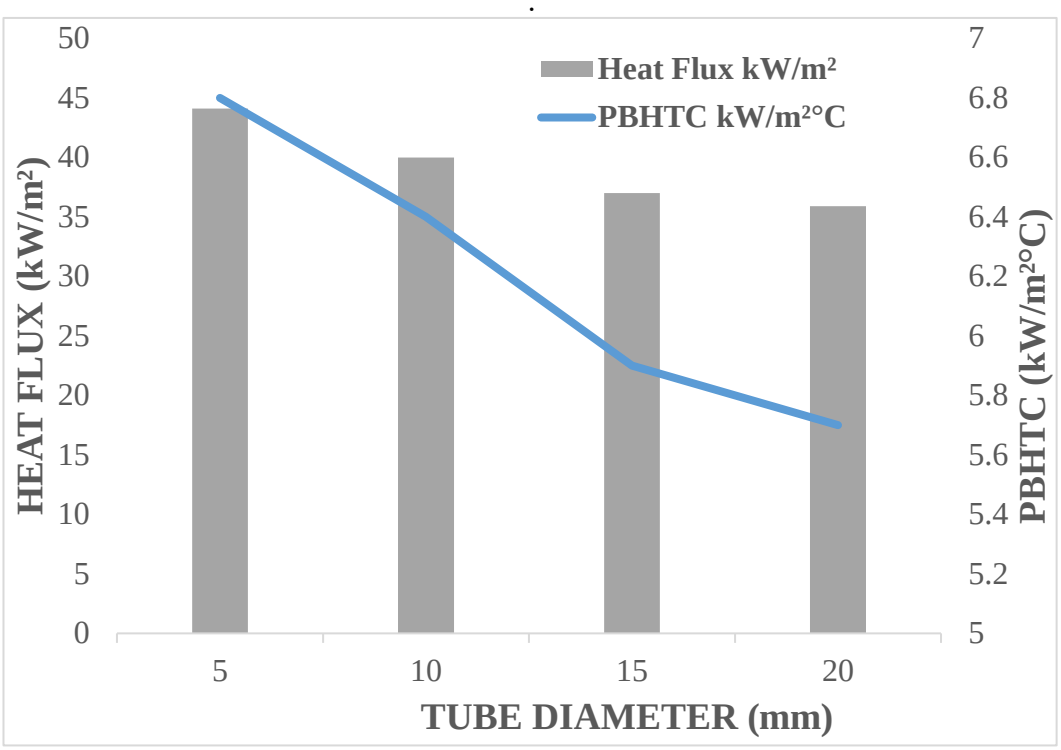

Figure 6.4: Heat flux and PBHTC values for different diameters based on 6.5°C superheat temperature.

In **Figure 6.4**, it is evident that with the increase in tube diameter, there is a gradual increase in the diameter at which bubble detachment occurs, accompanied by a decrease in both heat flux and the duration of bubble growth. The increase in bubble population heralds a decrease in heat flux, as the formation of bubbles entails the creation of a gas layer that behaves akin to insulation during its formation.

Diamater	0.3 s	0.4 s	0.5 s
5 mm	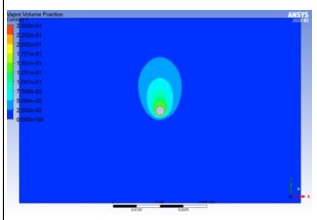	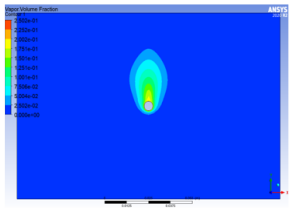	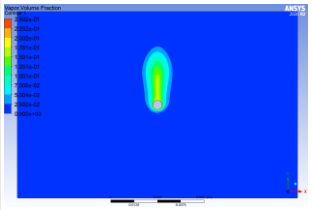
10 mm	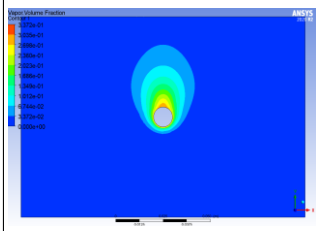	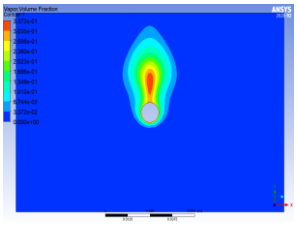	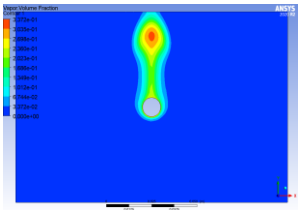
15 mm	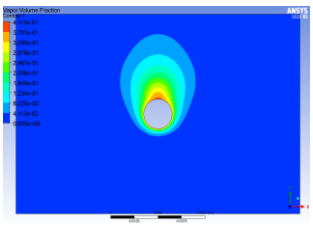	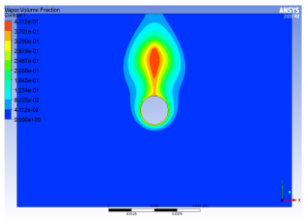	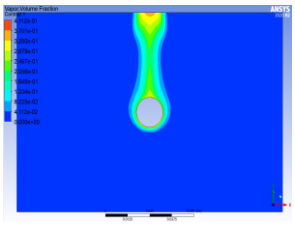
20 mm	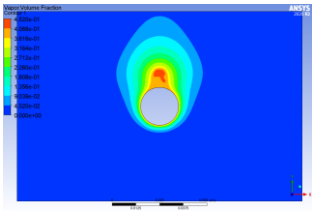	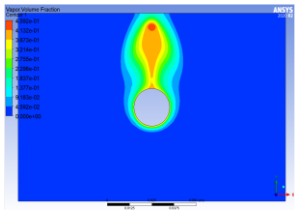	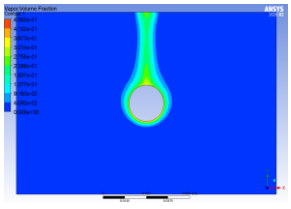

Figure 6.5: Bubble forming around different tube diameters (volume fraction) based on 6.5°C superheat temperature.

The investigation regarding hydrogen film boiling on tubes with different diameters studied by Jiaojiao et al. [28] shows decreasing in heat flux and bubble diameter with increasing tube diameter, **Figure 6.6**.

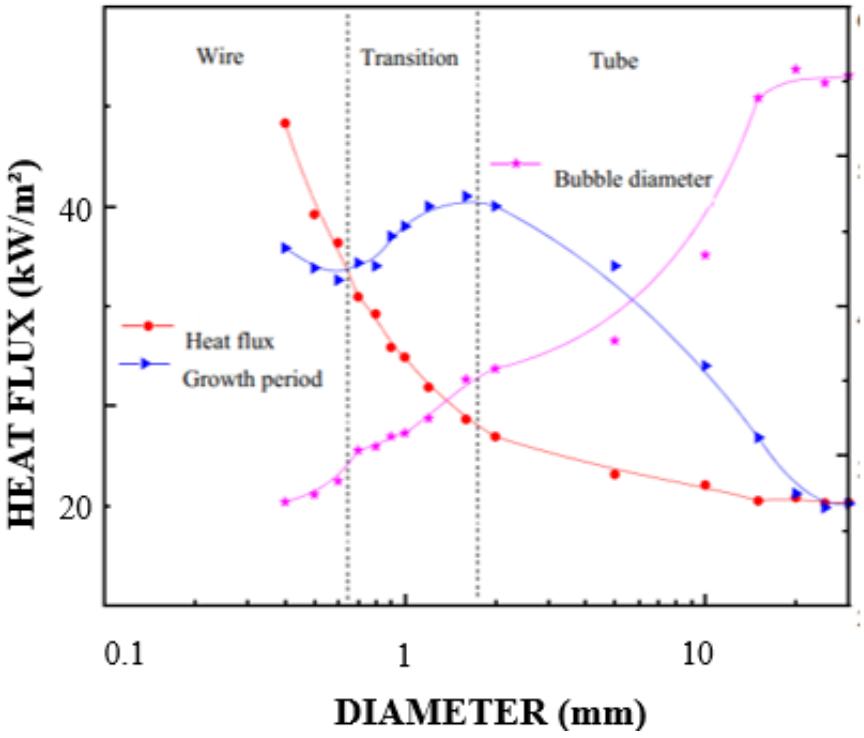

Figure 6.6: Averaged heat flux, bubble diameter, and growth period based on different diameters from Jiaojiao's **[28]** study.

6.3. Boiling at Atmospheric and Sub-atmospheric Pressure

In this research endeavor, the phenomenon of boiling on a horizontal pipe has been meticulously investigated under both atmospheric and sub-atmospheric pressures. The study encompasses an in-depth analysis of bubble behavior alongside the examination of heat flux and PBHTC values. In the process of evaluating the outcomes, insights gleaned from the work of Xue-Fei Yang and Zhen-Hua Lia [29] concerning the boiling of nano-fluids under sub-atmospheric conditions have been leveraged. Notably, it has been ascertained that similar findings were obtained, thereby enriching the comprehensiveness of the present investigation.

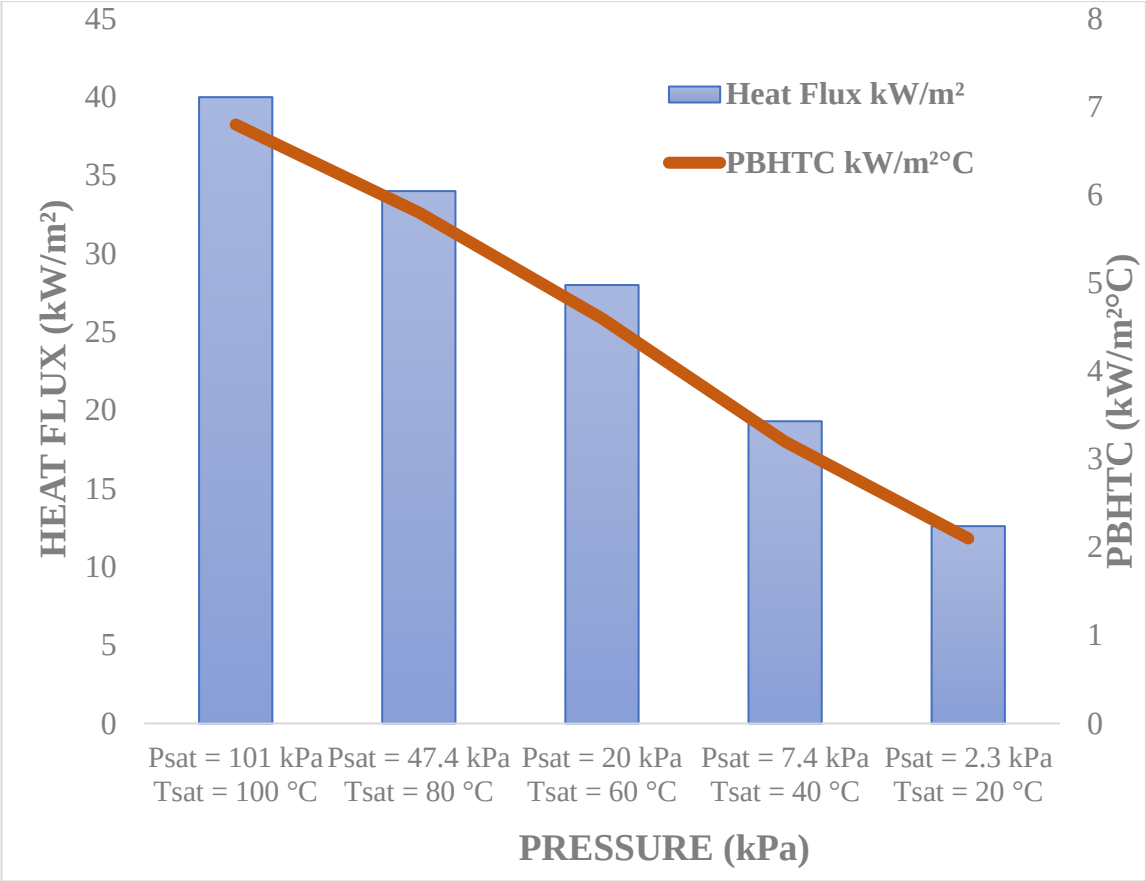

Figure 6.7: Heat Flux and PBHTC values on 10 mm diameter tube at atmospheric and sub-atmospheric pressure at superheat temperature 6.5°C.

In **Figure 6.7**, a discernible trend emerges where a reduction in pressure, indicative of a decrease in the saturation temperature of water, correlates with a subsequent decline in both the heat flux and PBHTC values observed on the horizontal tube surface. For the CFD study, the superheat temperature has been maintained at a constant value of 6.5°C. This observed diminishment can be comprehensively understood through the intricate interplay of water's thermodynamic properties. The reduction in pressure influences the saturation temperature of water, leading to alterations in its phase behavior and thermal conductivity. Consequently, this altered state impacts the mechanisms governing heat transfer phenomena on the pipe surface. Furthermore, the dependence of heat flux and PBHTC values on pressure underscores the significance of considering thermodynamic principles in elucidating the observed trends in boiling behavior.

In their study on both water and nanofluids on flat surfaces under different pressure conditions, Xue-Fei Yang and Zhen-Hua Liu [29] examined how the heat flux values change for both fluids. They found that as the pressure decreases, the heat flux on the flat surface also decreases. **Figure 6.7** illustrates this trend, and the trend matches with the present study.

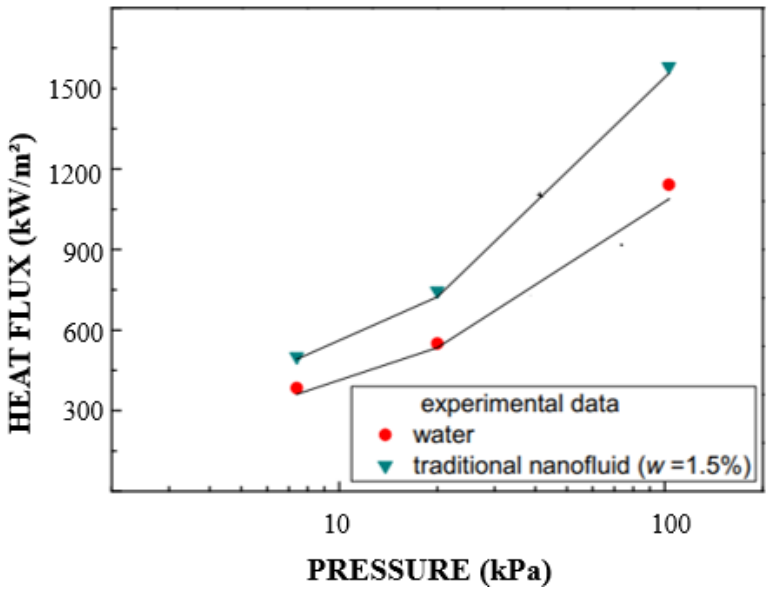

Figure 6.8: Heat flux values based on different pressures for water and nanofluid from Xue-Fei Yang and Zhen-Hua Liu's **[29]** study.

Figure 6.9-Figure 6.13 serves as illustrative depictions showcasing the phenomenon of bubble formation with volume fraction under different outlet pressure conditions. The results obtained in this section regarding bubble behavior under various pressures align with the study conducted by Sanra et al. [29]. Specifically, it becomes evident that as the outlet pressure is reduced, there is a notable increase in the duration of both bubble formation, growth, and detachment processes. The main explanation behind this finding is the alterations of both liquid and vapor densities of water, which are contingent upon the saturation pressure. By reducing the pressure within the specified pressure range, the liquid density (ρ_l) increases by approximately 4%, while the vapor density (ρ_v) demonstrates a significant reduces roughly 97%.

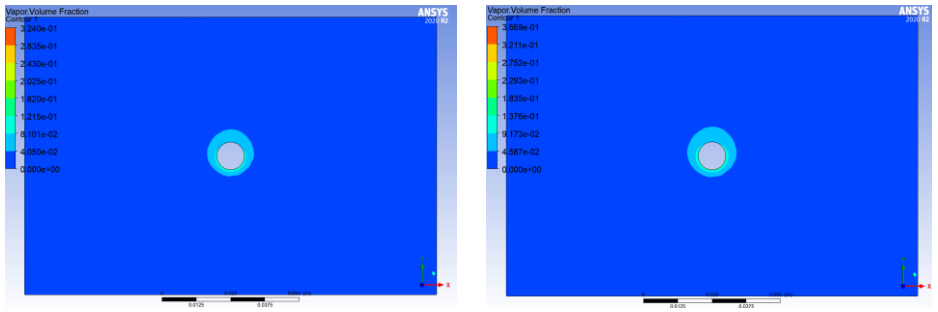

a) b)

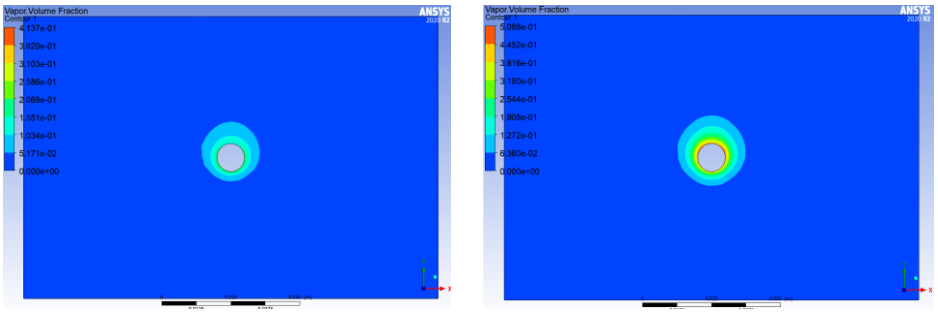

c) d)

Figure 6.9 The visual depiction of bubbles at different outlet pressures at 0.1second a)P_{sat}=101 kPa, b)P_{sat}=47.4kPa, c)P_{sat}=20 kPa, d)P_{sat}=7.4 kPa

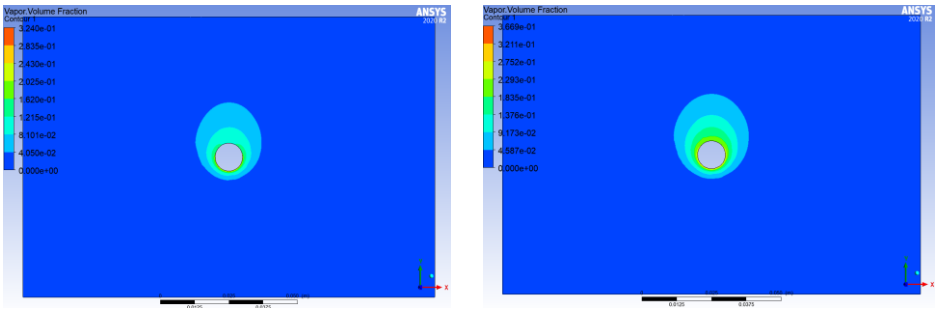

a) b)

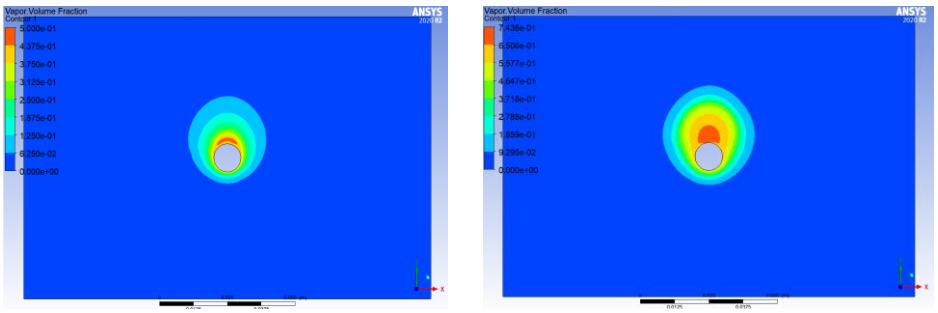

c) d)

Figure 6.10 The visual depiction of bubbles at different outlet pressures at 0.2second a)P_{sat}=101 kPa, b)P_{sat}=47.4kPa, c)P_{sat}=20 kPa, d)P_{sat}=7.4 kPa.

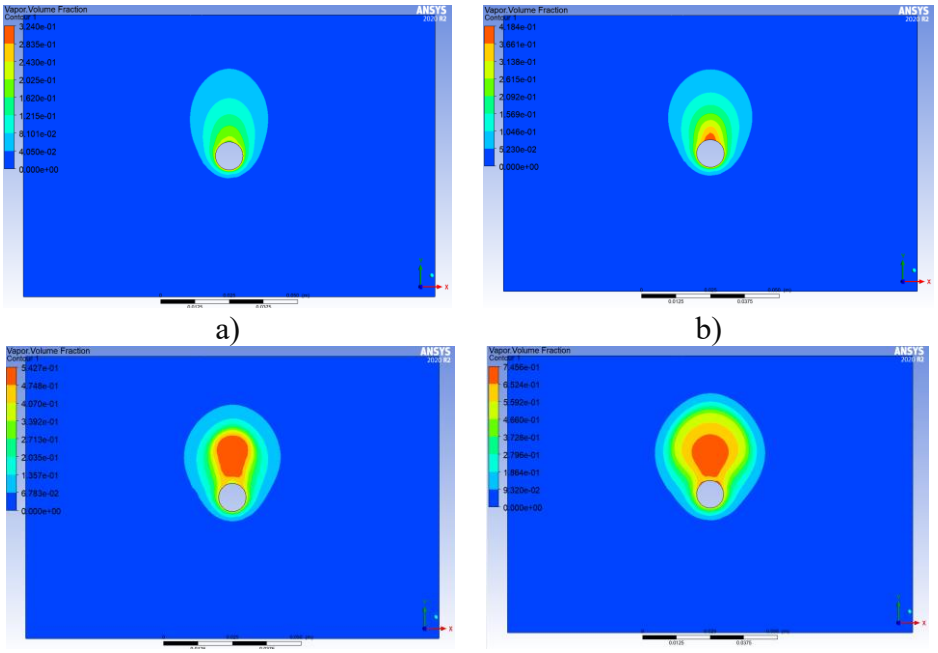

Figure 6.11 The visual depiction of bubbles at different outlet pressures at 0.3second a)P_{sat}=101 kPa, b)P_{sat}=47.4kPa, c)P_{sat}=20 kPa, d)P_{sat}=7.4 kPa

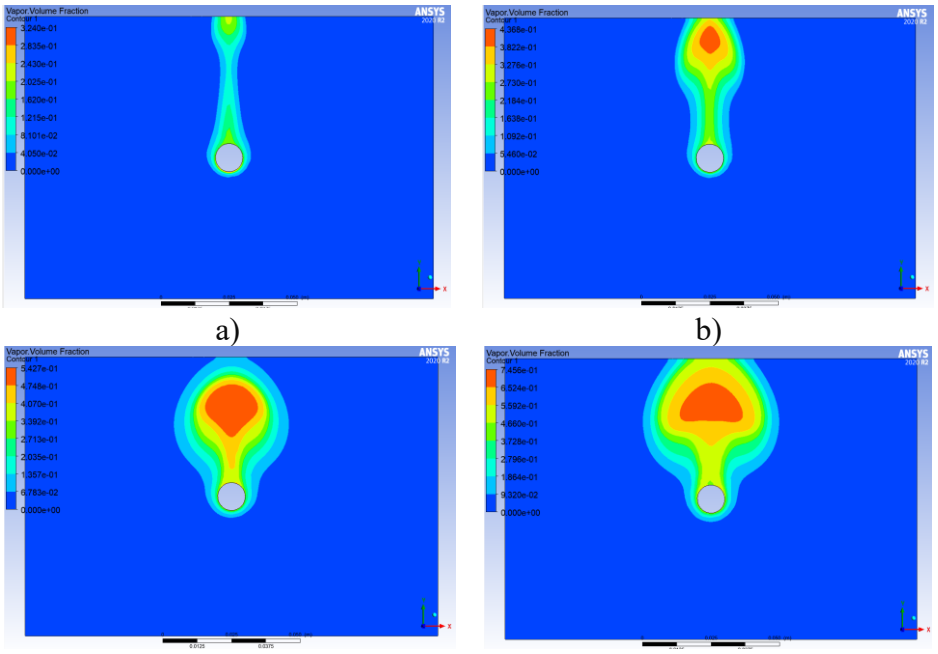

Figure 6.12 The visual depiction of bubbles at different outlet pressures at 0.5second a)P_{sat}=101 kPa, b)P_{sat}=47.4kPa, c)P_{sat}=20 kPa, d)P_{sat}=7.4 kPa

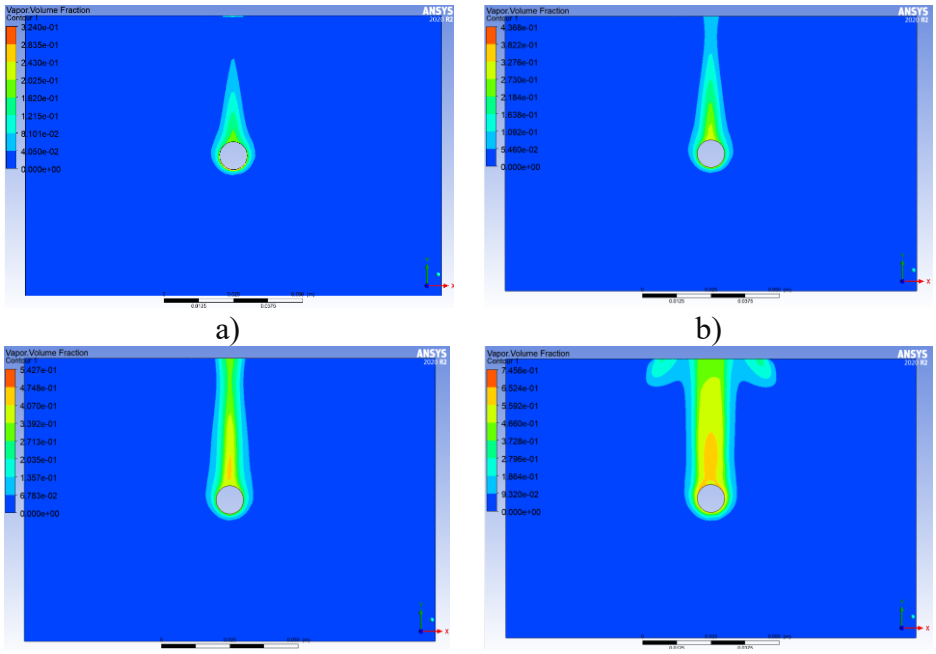

Figure 6.13 The visual depiction of bubbles at different outlet pressures at 0.7second a)P_{sat}=101 kPa, b)P_{sat}=47.4kPa, c)P_{sat}=20 kPa, d)P_{sat}=7.4 kPa

Moreover, concomitant with this reduction in process duration, there is an observable increase in the maximum diameter of bubbles, particularly noticeable at lower pressure regimes. This observation underscores the intricate relationship between outlet pressure variations and the dynamics of bubble formation and growth within the system under investigation. In **Figure 6.11**, there is a visual representation depicting the maximum diameters of bubbles that occurred. It is evident from the visualization that as the pressure decreases, the diameter of the bubble from the tube surface increases, aligning with the findings of the Santra et al. study [30]. They experimented with investigating bubble dynamics on a flat plate during pool boiling under both atmospheric and sub-atmospheric pressures, and **Figure 6.14** illustrates the results.

.

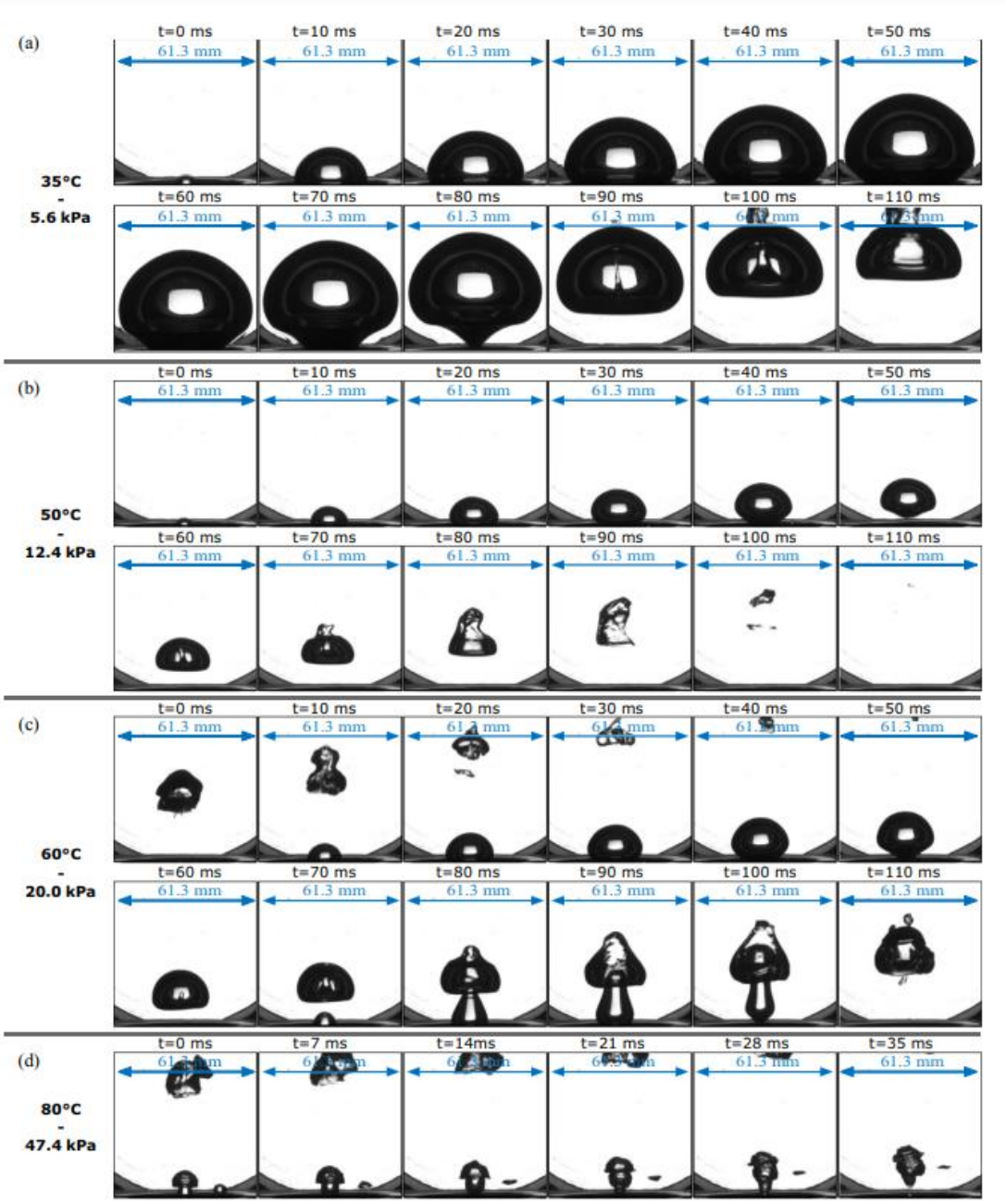

Figure 6.14: Bubble growth formation from Santra's **[30]** study.

This phenomenon can be attributed to the relationship between surface tension and contact pressure, as well as the resultant triple line forces, collectively termed the surface tension force. Consequently, the escalation of surface tension with decreasing saturation pressure poses challenges to bubble detachment, resulting in prolonged bubble growth durations and larger maximum volumes at lower pressures compared to higher pressures.

7. CONCLUSION

In this thesis, a wide range of topics related to pool boiling has been explored. Primarily, the thesis aims to investigate the nucleate boiling phenomenon on the surface of a horizontal tube. In the literature, there exist numerous experimental studies and computational fluid dynamics analyses regarding boiling. Given the multitude of factors influencing the boiling process, such as surface geometry, vacuum or pressurization, and the type of fluid used, there is noticeable diversity in the studies conducted. In this thesis, the behavior of boiling and bubbles on a tube surface has been analyzed using ANSYS Fluent software. Contrary to the widely recognized VOF model, the Euler-Rensselaer Polytechnic Institute (RPI) model has been employed due to the complexity of the subject matter. Initially, an appropriate model was identified from the literature and subsequently validated. The heat flux and PBHTC values observed by Mohammed Saad for different superheat temperatures on a constant tube diameter were adopted as a model. Following the validation process, necessary modifications were made, and observations were made on how parameters such as heat flux and PBHTC vary across different tube diameters. Subsequently, the variations in heat flux and heat transfer coefficient values on a constant tube diameter due to the boiling of vacuumed water on the tube surface were examined. Not only numerical values but also bubble behaviors under different tube diameters and pressure conditions were investigated. The accuracy of the values and bubble behaviors was compared with the results of experimental studies in the literature, thereby ensuring the reliability of the obtained results and the predictive capability thereof.

Through the extensive CFD study conducted, the following results have been obtained:

- As the tube diameter increases, a decrease in both heat flux and PBHTC has been observed. Flux is reduced by 55 % when the diameter is increased from 5 mm to 20 mm.
- With increasing tube diameter, the volume of bubbles formed also increases.
- As the tube diameter increases, the duration of bubble formation, growth, and detachment processes decreases.
- Decreases in pressure, corresponding to a vacuum environment, lead to a decrease in heat flux on the tube surface, along with a reduction in the PBHTC.

Heat flux is reduced by 70 % when pressure is reduced from 101 kPa to 2.3 kPa.

- A notable increase in bubble size is observed with decreasing pressure.
- Decreases in pressure result in elongation of the bubble formation, growth, and detachment processes from the surface.

In future investigations within this thesis topic, the computational fluid dynamics results can be augmented and substantiated by experimental studies. In this thesis, water is utilized as the primary fluid medium; however, alternate fluids such as hydrogen could be employed, enabling a comparative analysis of pool boiling phenomena.

REFERENCES

[1] Jawsal R., Sathyabhama A., Singh K., Yandapalli Prasad A.V.V.R., (2023), "Experimental and Numerical Investigation of Pool Boiling Heat Transfer from Finned Surfaces", Applied Thermal Engineering, 233 (2023), 121-167.

[2] Kamel Saad M., Lezsovits F., (2020), "Numerical and Experimental Investigation on Pool Boiling Heat Transfer Performance using Nanofluids", Journal of Advanced Research in Fluid Mechanics and Thermal Sciences, 71(2), 35-55.

[3] Sajjad U., Hussain I., Sultan M., Mehdi S., Wang C., Rasool K., Saleh M. S., Elnaggar A., Hussein E. E., (2021), "Determining the Factors Affecting the Boiling Heat Transfer Coefficient of Sintered Coated Porous Surfaces", Sustainability, 13(22), 12631.

[4] Nukiyama S., (1966), "Maximum and Minimum Values of Heat Transmitted From Metal to Boiling Water Under Atmospheric Pressure", International Journal of Heat and Mass Transfer, 9(2), 1419-1433.

[5] Kim D. E., Yu D., Jerng D. W., Kim M. H., Ahn H. S., (2015), "Review of boiling heat transfer enhancement on micro/nanostructured surfaces", Experimental Thermal and Fluid Science, 66, 173-196.

[6] Bian H., Cheng K., Kurwitz C., Chen K., (2018), "Enhanced nucleate boiling on 3D-printed micro-porous structured surface", Applied Thermal Engineering, 141, 422-434.

[7] Sateesh G., Das S. K., Balakrishnan A. R., (2005), "Analysis of pool boiling heat transfer: effect of bubbles sliding on the heating surface", International Journal of Heat and Mass Transfer, 48, 1543–1553.

[8] Kim J. S., Kim Y., Cho H. K., (2020), "Predicting the sliding bubble velocity on the lower part of a horizontal tube heater under natural convection based on force balance analysis'', International Journal of Heat and Mass Transfer, 15, 19453.

[9] Kim J., (2009), " , International Journal of Multiphase Flow, 35, 1067–1076.

[10] Zou A., Gupta M., Maroo S., (2018), "Origin, Evaluation, and Movement of Microlayer in Pool Boiling'', The Journal of Physical Chemistry Letters, 9, 3863-3869.

[11] Guichet V., Mahmoud S., Jouhara H., (2019), "Nucleate pool boiling heat transfer in wickless heat pipes (two-phase closed thermosyphons: a critical review of correlations'', Thermal Science and Engineering Progress, 13(9), 100384.

[12] Gorgy E., Eckels S., (2012), "Local heat transfer coefficient for pool boiling of R-134a and R-123 on smooth and enhanced tubes'', International Journal of Heat and Mass Transfer, 55, 3021-3028.

[13] Chien L. H., Webb R. L., (1998), "A parametric study of nucleate boiling on structured surfaces'', International Journal of Heat and Mass Transfer, 120(4), 1042-1048.

[14] Ribatski G., Thome J. R., (2007), "Two-phase flow and heat transfer across horizontal tube bundles-a review'', Heat Transfer Engineering, 28(6), 508–524.

[15] Gorenflo D., Baumhögger E., Windmann T., Herres G., (2010), "Nucleate pool boiling, film boiling and single-phase free convection at pressures up to the critical state'', International Journal of Refrigeration, 33, 1229–1250.

[16] Yagov V. V., Gorodov A. K., Labuntsov D. A., (1970), "Experimental study of heat transfer in the boiling of liquids at low pressures under conditions of free motion'', Journal of Engineering Physics and Thermophysic, 18, 421–425.
[17] Abadi N. R., Ahmadpour A., Meyer J. P., (2018), "Numerical simulation of pool boiling on smooth, vertically aligned tandem tubes'', International Journal of Thermal Sciences, 132, 628-644.

[18] Rohsenow W. M., (2011), "A method of correlating heat transfer data for surface Boiling of liquids'', Journal of Fluids Engineering, 74(6), 969-975.

[19] Forster H. K., Zuber N., (1955), "Dynamics of vapor bubbles and boiling heat transfer'', AlChe Journal, 1(4),531- 535.

[20] Borishansky V. M., (1696), "Correlation of the effect of pressure on critical heat flux and heat transfer rates using the theory of thermodynamic similarity'', Problems of Heat Transfer and Hydraulics, 16-37.

[21] Kurul N., Padowski M., (1990), "Multidimensional effects in forced convection subcooled boiling'', International Heat Transfer Conference 9, 2377-424X, Jerusalem, Israel, 19-24 August 1990.

[22] Yoo J., Estrada-Perez C. E., Hassan Y. A., (2018), "Development of a mec hanistic model for sliding bubbles growth prediction in subcooled boiling flow'', Applied Thermal Engineering, 138, 657-667.

[23] Unal H. C., (1976), "Maximum bubble diameter, maximum bubble-growth time and bubble-growth rate during the subcooled nucleate flow boiling of water up to 17.7 MN/m2'', International Journal of Heat and Mass Transfer, 19(6), 643-649.
[24] Basu N., Warrier G. R., Dhir V. K., (2005), "Wall heat flux partitioning during subcooled flox boling'', International Journal of Heat and Mass Transfer, 127(2), 131-140.

[25] Maity S., Dhir V. K., (2001), "An experimental study of vapor bubble dynamics on inclined surfaces subjected to forced flow along the surface'', 35th National Heat Transfer Conference, Anaheim, CA, USA, 2001.

[26] Kamel M. S., (2020), "Numerical and Experimental Investigation on Pool Boiling Heat Transfer Performance Using Nanofluid'', Ph.D. Thesis, Budapest University of Technology and Economics.

[27] Setoodeh H., Ding W., Lucas D., Hampe U., (2019), “Prediction of bubble departure in forced convection boiling with a mechanistic model that considers dynamic contact angle and base expansion’’, Energies, 12(10), 1950.

[28] Wang J., Li Y., Wang L., (2022), “Numerical study on pool film boiling of liquid hydrogen over horizontal cylinders’’ Energies, 15(13), 1044.

[29] Yang X., Liu Z., (2011), “Pool boiling heat transfer of functionalized nanofluid under sub-atmospheric pressures’’, International Journal of Thermal Sciences, 50(12), 2402-2412.

[30] Michaie S., Rullière R., Bonjour J., (2016), “Experimental study of bubble dynamics of isolated bubbles in water pool boiling at subatmospheric pressures’’, Experimental Thermal and Fluid Science, 87, 117–128.

BIOGRAPHY

My name is Sinan OZBOLGILI. I obtained my degree from the Department of Mechanical Engineering at Yildiz Technical University in 2014, with a primary focus on thermal and processing systems. Following my graduation, I pursued further studies in the English language at Georgia Tech University for a period of six months. Subsequently, I served as a development engineer at Systemair Turkey, a prominent manufacturer of HVAC units, for a duration of four years. During this tenure, my responsibilities were primarily centered around the development of moisture control units featuring heat pump technology. Presently, I am employed as a development engineer specializing in chillers and HVAC systems at SKM Air Conditioning LLC company in Dubai, where I have successfully completed my fifth year of service.

PUBLICATIONS AND PRESENTATIONS FROM THE THESIS

Ozbolgili S., Gediz Ilis G., (2024), “Computational Investigation of Pool Boiling Around Different Diameter Horizontal Tubes Under Atmospheric and Sub-Atmospheric Pressure”, Gebze, Türkiye, 30-31 May.